Appendix J
Wind Impact on Cable Tensions

1.0 Introduction

Tropical storms and hurricanes regularly impact the island of Puerto Rico in the summer months, which can subject the telescope to high sustained and fluctuating wind loads. Our analysis of the wind loads effects on the telescope's cable system is presented in this appendix.

The highest instantaneous wind speed ever recorded at Arecibo Observatory is 110 mph and occurred as the eye of Hurricane Maria approached the site on September 20, 2017. While the hurricane caused widespread destruction in Puerto Rico, the only significant damage reported on the telescope was a failure of the line feed (Figure 1). However, because of the relatively short time between Hurricane Maria and the telescope's first cable failure (August 10, 2020), it is natural to investigate the storm as a potential factor contributing to the collapse. Hurricane Maria is therefore used as a reference load throughout our analysis of the wind load effects.

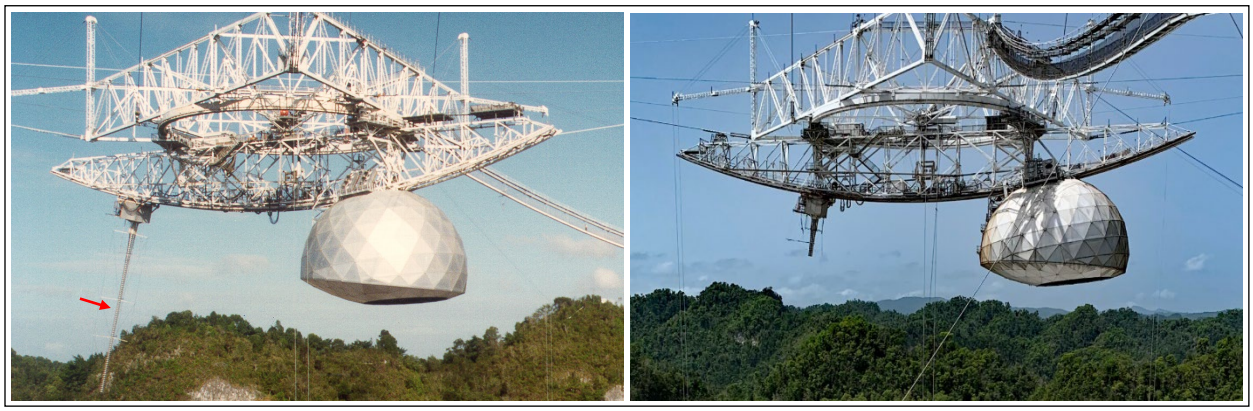

Figure 1: Suspended structure before (left) and after (right) Hurricane Maria, with damage to the line feed
(left photo: NAIC Arecibo Observatory, a facility of the NSF;
right photo: Mario Roberto Duran Ortiz, Wikipedia - CC By-SA 4.0).

2.0 Design Considerations

We reviewed the structural design documents and associated correspondence produced during the construction and upgrades of the telescope. Our findings are summarized in this section.

2.1 Design Wind Speed

The documents we reviewed indicate that different wind speeds were considered for the design of the original structure and the two upgrades.

The structural drawings for the original structure[1] indicate a design wind speed of 140 mph. Before the first upgrade of the telescope, a feasibility study by Ammann & Whitney (AW)[2] determined that the speed of 140 mph corresponds to the 300-year wind event at the telescope's site, and that the 100-year wind speed is only 114 mph.

[1] Praeger-Kavanagh. Structural drawings for original telescope. December 1, 1960. Drawings provided by Arecibo Observatory.

[2] Ammann & Whitney. *Feasibility Study and Concept Development for Upgrading of Suspended Antenna Structure*. August 1972. Report retrieved from Cornell University archives.

AW's structural drawings for the first upgrade[3] indicate a design wind speed of 110 mph, suggesting that the 100-year wind event was selected as design event.

Before the second upgrade of the telescope, the design wind speed was discussed between AW (engineer of record), Radiation Systems Inc (RSI, prime contractor for the upgrade), Temcor (engineer for the Gregorian), and West Wind Laboratory (WWL, contracted to perform a wind tunnel study of the Gregorian). AW had specified a wind speed of 100 mph for the design of the second upgrade,[4] but WWL's report on the wind tunnel test of the Gregorian included a recommendation to use a much higher speed of 153 mph.[5] AW increased the design wind speed to 110 mph based on newly available data but dismissed the 153 mph recommendation as too conservative and based on an unsolicited study by WWL.[6] AW also clarified that 110 mph would be used for the global structural design of the upgrade, which includes the calculation of cable tensions, while Temcor may consider a higher wind speed as deemed appropriate for the local design of the Gregorian enclosure. WWL maintained their recommendation of 153 mph but also determined that the Gregorian enclosure should be designed for 123 mph[7] to be consistent with the 110 mph selected by AW for the global structural design. AW confirmed the two speeds of 110 mph and 123 mph for the global and local design of the upgrade respectively[8] and, to our knowledge, the final design was based on those wind speeds.

2.2 Design Wind Load and Cables Tensions

The structural drawings for the original and upgraded structures indicate the maximum cable tensions calculated under dead load and the combination of dead load and design wind load. These tensions are summarized in Table 1, where the relative tension increase due to wind is also calculated. While wind increases the cable tensions by up to 26 percent in the original structure, the increase is less than six percent in the upgraded structure. This difference is due to three factors. First, the design wind speed was lowered from 140 mph to 110 mph between the original design and the second upgrade (section 2.1 above). Then, the second upgrade added 12 cables to the system, such that more cables shared the wind load. And finally, the design of the upgraded structure assumes that the tiedown cables between the platform and the ground are partially released before the arrival of a significant storm, purposefully to reduce the cable tensions.

From the cable tensions provided in the drawings and the known geometry of the cable system, we back-calculated the total design wind load on the suspended structure. The calculation assumes that the maximum tension in a cable occurs when the wind blows in the cable's direction towards the suspended structure (e.g. the maximum tension in the Tower 12 mains occurs when the wind blows south). The suspended structure is assumed rigid, and the wind load is assumed horizontal only (no uplift or downdrag). The pre-storm tiedown release is taken

[3] Ammann & Whitney. Structural drawings for first upgrade of telescope. October 20, 1972. Drawings retrieved from Cornell University archives.

[4] Amman & Whitney. Structural drawings for second upgrade of telescope. 1992. Drawings provided by Arecibo Observatory.

[5] West Wind Laboratory, Inc. *Wind Study of Arecibo Radio Observatory*. December 1993. Report retrieved from Cornell University archives.

[6] Joseph Vellozzi (Ammann & Whitney). Letter to William Terry (Radiation Systems Inc). January 18, 1994. Correspondence retrieved from Cornell University archives.

[7] Jon Raggett (West Wind Laboratory, Inc). Letter to Alfonso Lopez (Temcor). January 31, 1994. Correspondence retrieved from Cornell University archives.

[8] Joseph Vellozzi (Ammann & Whitney). Letter to Walter Marusak (Radiation Systems Inc). March 8, 1994. Correspondence retrieved from Cornell University archives.

into account in the upgraded structure. We determined a total design wind load of 675 kilopound (kip) for the original structure and 444 kip for the upgraded structure (Figure 2).

Before the second upgrade, a wind tunnel study was performed on the Gregorian dome (section 2.3 below). However, we found no record of any wind tunnel study on the steel trusses making up the rest of the suspended structure. Therefore, it is likely that the wind loads on the trusses were determined analytically. This is typically done through some variant of a drag calculation where the wind load is proportional to the square of the wind speed and to the structure's area modified by a drag coefficient. From the design wind speed and load previously determined, we back-calculated the effective product of drag coefficient and surface area (Table 2). We note that this quantity increases by only 7 percent between the original to upgraded structures, even though the Gregorian dome adds significant surface area. This may be explained by the lower drag coefficient of the Gregorian dome compared to steel trusses and possibly the use of different assumptions in the calculation of the load on the steel trusses.

Table 1: Design wind load and cable tensions in structural drawings of original and upgraded telescope.

		Original Structure			Upgraded Structure		
		Dead Load Only [kip]	Dead Load + Design Wind [kip]	Relative Increase due to Wind	Dead Load Only [kip]	Dead Load + Design Wind [kip]	Relative Increase due to Wind
Original Cables	Mains	527	642	+22%	480	496	+3%
	Tower 4 Backstays	593	748	+26%	543	577	+6%
	Tower 8 Backstays	541	682	+26%	503	532	+6%
	Tower 12 Backstays	566	696	+23%	514	540	+5%
Auxiliary Cables	Mains	-	-	-	602	622	+3%
	Tower 4 Backstays	-	-	-	728	769	+6%
	Tower 8 Backstays	-	-	-	662	698	+5%
	Tower 12 Backstays	-	-	-	727	760	+5%

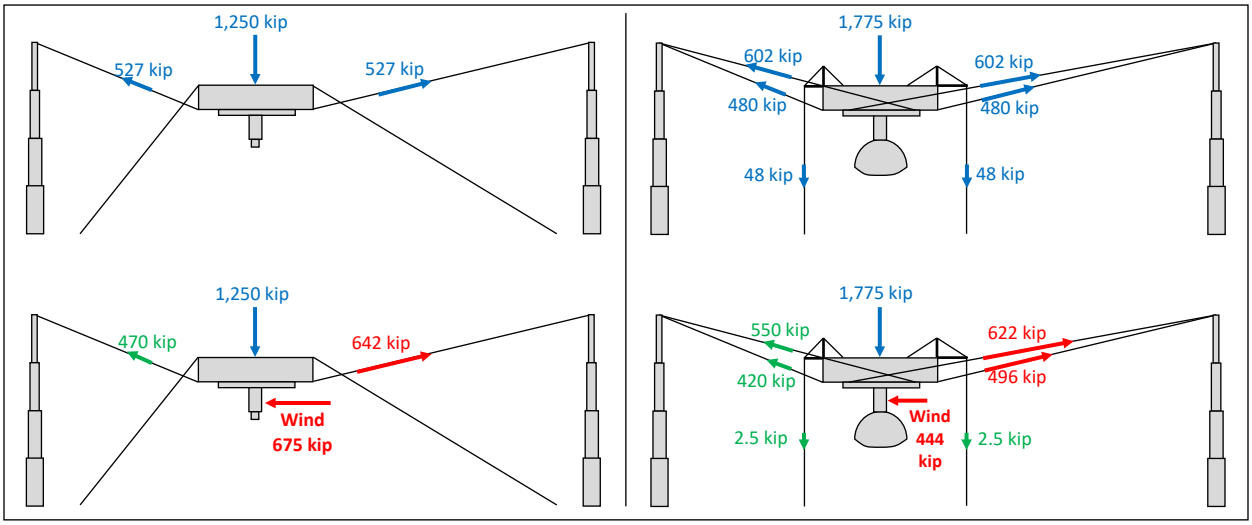

Figure 2: Equilibrium of original (left) and upgraded (right) structures under design wind load and cable tensions.

Table 2: Design wind load information derived from structural drawings.

	Original Structure	Upgraded Structure
Design Wind Speed [mph]	140	110
Design Wind Load [kip]	675	444
Effective Drag Coefficient x Area[A] [ft²]	13,480	14,360

[A] Calculated as F / (0.5 ρ V²) where F is the wind load, ρ the mass density of air and V the wind velocity

2.3 Gregorian Wind Tunnel Test

A wind tunnel study was performed in 1993 as part of the engineering of the telescope's second upgrade. The study was conducted by West Wind Laboratory (WWL). Its objective was to determine the maximum wind pressures on the surface of the Gregorian dome, to be used by Temcor to design the dome enclosure. However, WWL also integrated the wind pressures over the dome's surface to determine the total wind loads on the dome, which are provided in their report. While we could not confirm all of the assumptions and parameters used by WWL, this wind tunnel study remains a valuable data point to compare to our calculations and computational fluid dynamic (CFD) analyses.

The wind tunnel tests relied on a typical method for testing large structures, where the structure's dimensions and the wind speed are both scaled-down. As long as the airflow in the test is still fully turbulent, as is for the full-size structure during a hurricane, the wind forces from the test can be scaled back to the full-size structure. Additional details are provided in section 5.1, where the same method is applied to CFD analysis results.

The tests were performed on a 1:125 scaled model (approximately 2.5 feet) of the suspended structure (Figure 3). While the model also included the platform and azimuth arm, only the Gregorian was equipped with pressure taps. At least three tests were performed with the wind coming from three different directions (Gregorian's front, back, and side). An additional test was performed on a cylinder with a diameter similar to Gregorian's model (Figure 3). The force on the cylinder was found to agree well with the expected drag force on a cylinder in a turbulent regime, confirming that the test regime was fully turbulent.

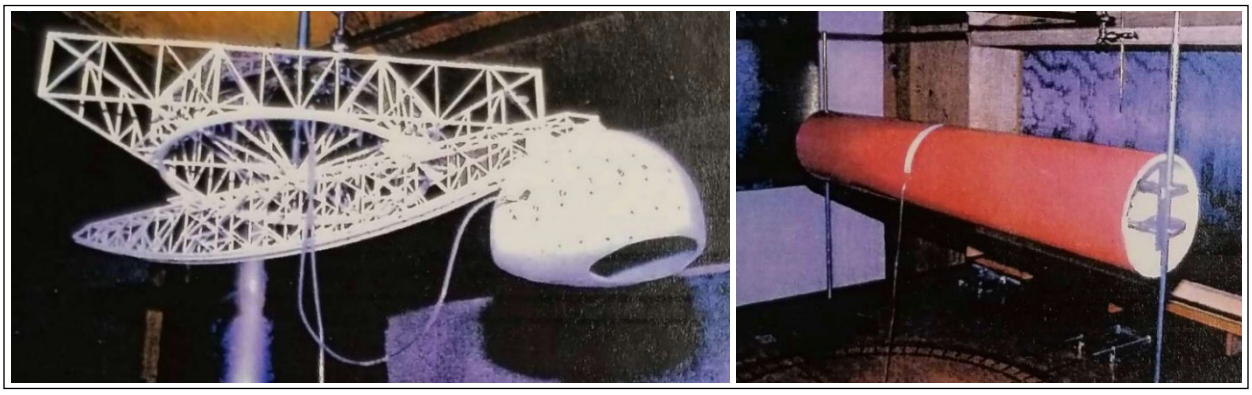

Figure 3: Model of suspended structure (left) and calibration cylinder (right) during 1993 wind tunnel tests. *(photos: West Wind Laboratory).*

The resultant forces on the Gregorian determined from the wind tunnel tests are presented in Figure 4, after scaling to the 110 mph design wind speed. An effective drag coefficient is then calculated in Table 3 for each wind direction.

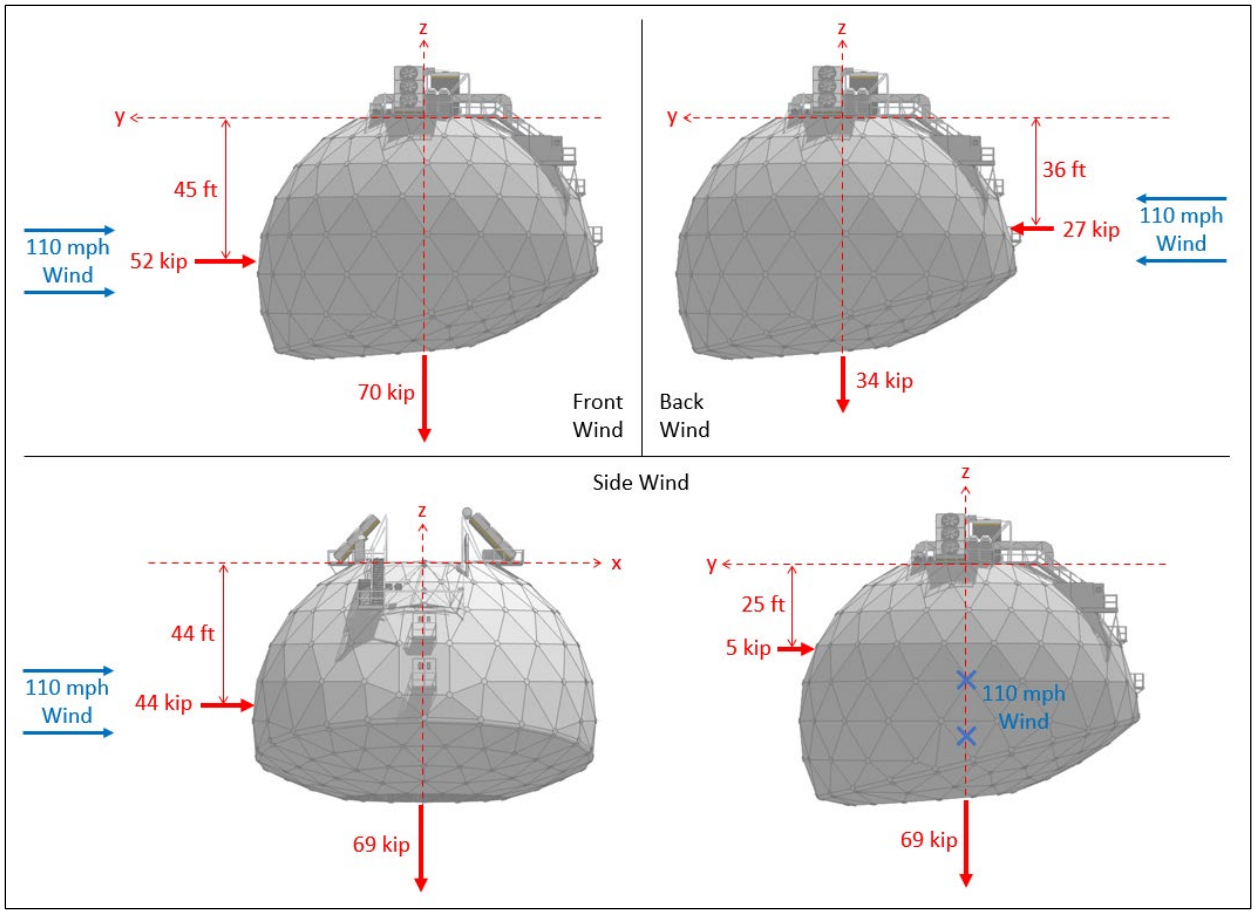

Figure 4: Gregorian wind tunnel test results, scaled to 110 mph wind speed *(images: Sketchup 3D Warehouse).*

Table 3: Gregorian effective drag coefficient calculation from wind tunnel test results.

Wind Speed V [mph]		110		
Air Mass Density ρ [lbf.s^2.ft^{-4}]		0.00238		
Dynamic Wind Pressure P = 0.5 ρ V^2 [psf]		31.0		
Wind Direction		From Front (-y)	From Back (+y)	From Side (±x)
Along Wind	**Wind Load F [kip]**	52	27	44
	Projected Area A [ft2]	3850	3850	3850
	Effective Drag Coefficient C = F / P / A	0.44	0.23	0.37
Cross Wind	**Wind Load [kip]**	0	0	5

3.0 Data

Our analysis of the telescope's response to wind loads relies on two sets of data recorded over time at the Observatory: the wind speed and direction and the telescope's tiedown tensions.

3.1 Wind Speed and Direction

The telescope's platform was equipped with a weather station that measured wind speed and direction, among other meteorological parameters (Figure 5). The wind speed was measured by two independent instruments: an anemometer and a doppler.

The doppler data was plotted by AO for several windstorms, such as Hurricane Maria, as shown in Figure 6. The plots show the wind slowing down to almost zero and reversing direction as the eye of the storm passes over the Observatory. We also note that the maximum instantaneous wind speed recorded during the storm is 108 mph, or two percent less than the second upgrade's design wind speed of 110 mph.

Figure 5: Location of weather station on suspended structure
(photo: Mario Roberto Duran Ortiz, Wikipedia - CC By-SA 4.0).

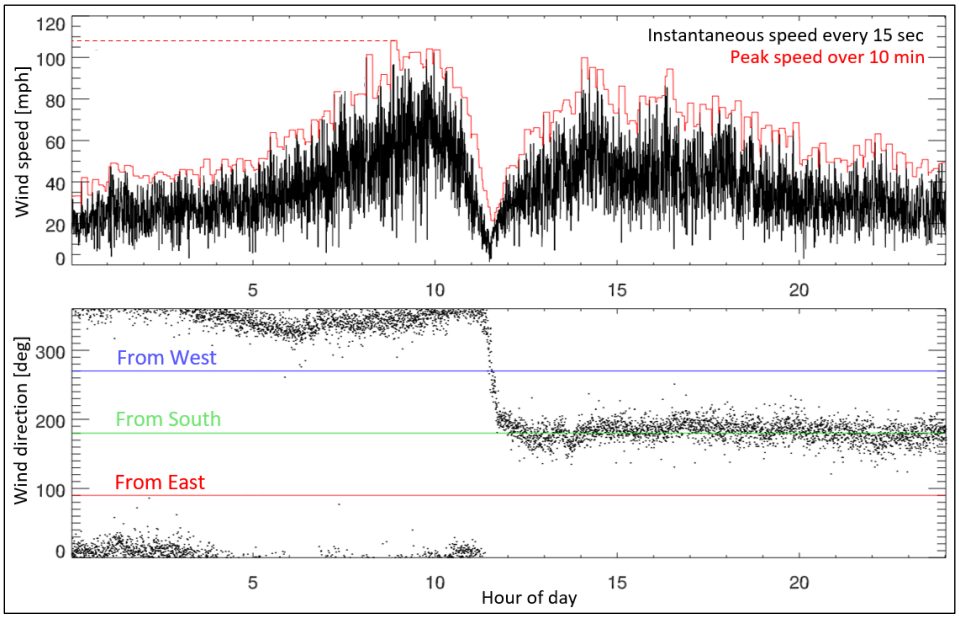

Figure 6: Wind speed and direction on suspended structure on September 20, 2017 as hurricane Maria passes over the Observatory *(images: NAIC Arecibo Observatory, a facility of the NSF).*

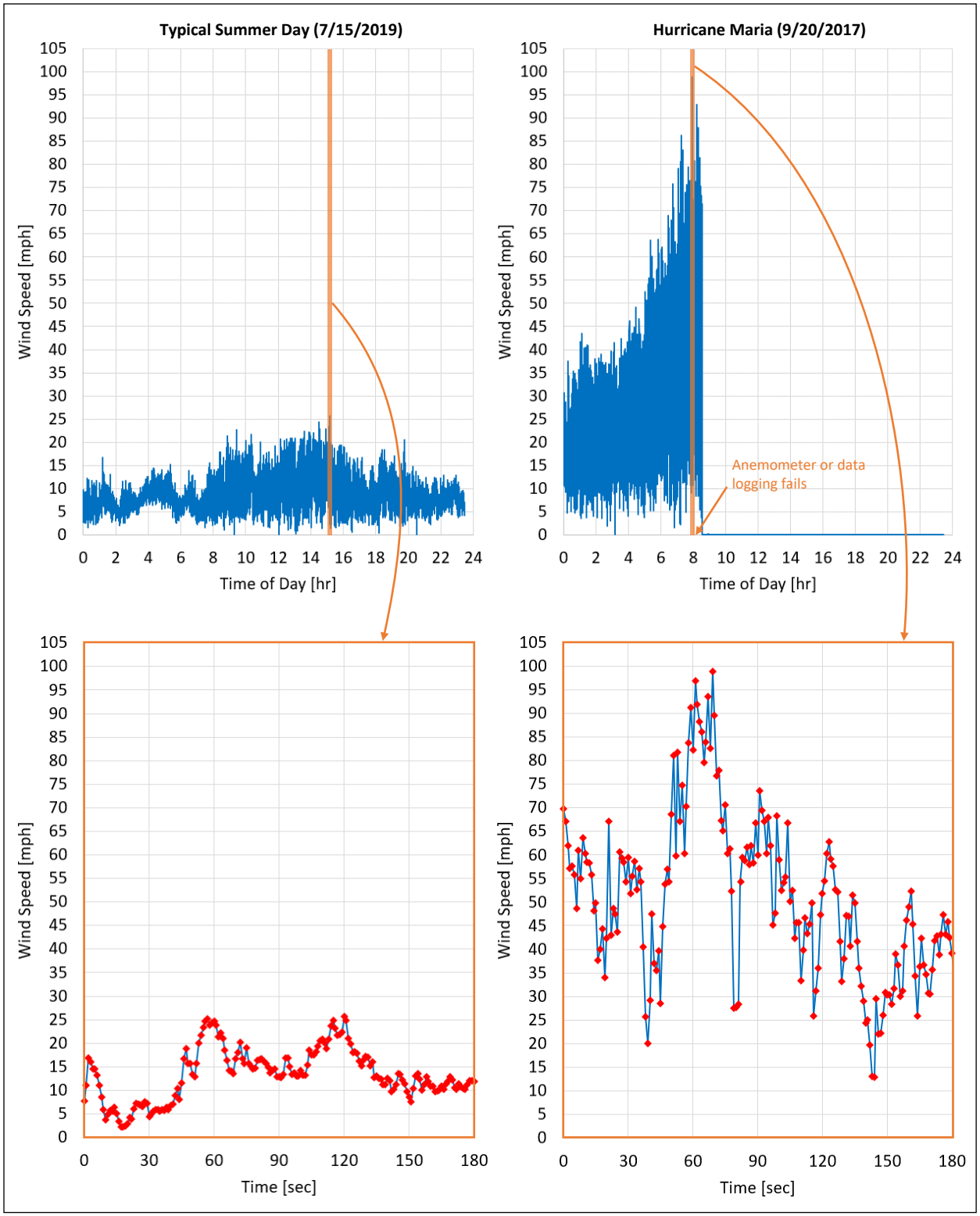

Figure 7: Wind speed recorded at one Hertz on a typical summer day and during Hurricane Maria.

The anemometer data was logged at one-second intervals from 2005 to the collapse in 2020, and the complete data set was provided to us by AO. While the data has gaps, likely due to power outages and equipment malfunctions, it captures several major windstorms and otherwise records the ambient wind on regular days. For two reasons, the anemometer data is particularly valuable to study the suspended structure's dynamic response to wind loads. First, it was measured directly on the suspended structure and therefore does not need to be scaled or modified to account for elevation or topographic effects. And second, it was recorded at shorter time intervals (one second) than the period of the structure's first mode of vibration (approximately three seconds), such that the wind's frequency content that could impact the structure's dynamic response is expected to be reasonably well captured in the data.

Excerpts of the anemometer data are provided in Figure 7 for a typical summer day and on the day of Hurricane Maria. The data for Hurricane Maria stops at 8:30 AM due to power loss or damage to the system.

3.2 Telescope Tiedown Tensions

The three tiedowns of the upgraded structure, which connected the platform to the ground, were equipped with load cells that measured the tiedown tensions continuously. Each tiedown consisted of two parallel cables, and each cable had its own load cell. The tiedown cable tensions were logged at one-second intervals since 2004, and the complete data set was provided to us by AO.

The tiedown tensions can be used to evaluate the vertical movement of the suspended structure during windstorms. While the tiedown tensions are usually affected by the tiedown jacks' action and the daily temperature cycles, the jacks were locked in place during storms and the temperature effects are much slower and easily discernable from wind-induced vibrations. A limitation is that the tiedown jacks were locked in an extended position to decrease the tiedown tensions and stress in the overall cable system. As a result, the tiedown tensions were relatively low during storms, which may affect the accuracy of the load cells.

The tiedown tensions recorded during Hurricane Maria are shown in Figure 8. For tiedowns 8 and 12, the tiedown tension is calculated as the sum of the tensions in the tiedown's pair of load cells. For tiedown 4, the tiedown tension is calculated as twice the tension in one of the load cells, as the other load cell recorded unrealistically high values even before the storm. Finally, the total tiedown tension is also calculated. We observe that the three tiedown tensions are generally synchronized and fluctuate at a three-second period (3 data points per cycle), which is consistent with the period of the suspended structure's first mode of vibration.

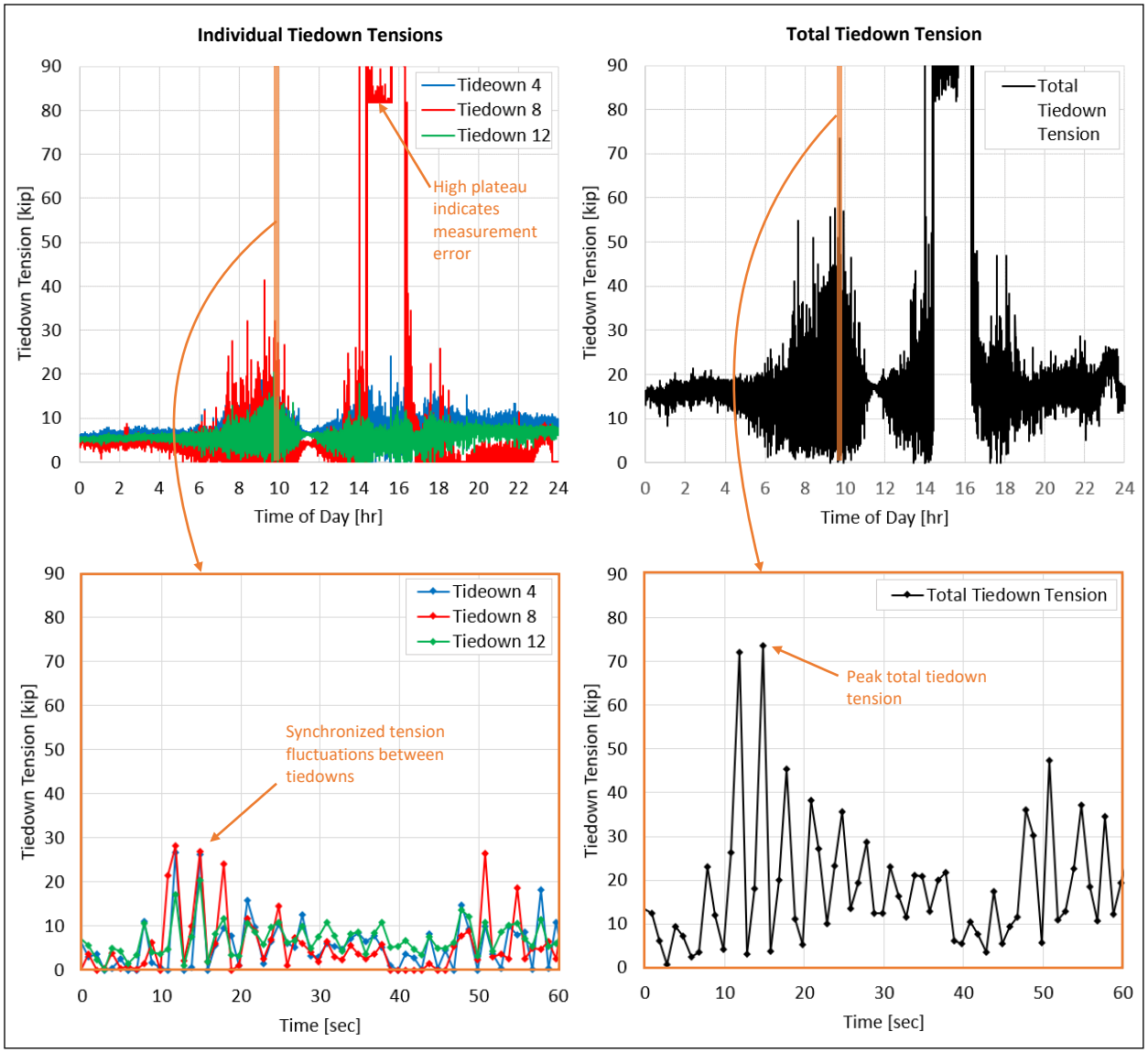

Figure 8: Tiedown tensions recorded during Hurricane Maria.

4.0 Static Wind Load Calculations

As a first analysis, we estimated the wind loads on the upgraded telescope through first-principle and standard structural design calculations. This type of calculation is inherently approximate, and the structure's unique features require making assumptions that increase the uncertainty on the results. Yet, those results remain a valuable basis for validating the more complex analyses presented in the rest of this appendix. All of the calculations presented in this section estimate the static wind load induced by the reference wind speed of 110 mph considered in this study.

4.1 Suspended Structure

4.1.1 Platform and Azimuth Arm

The platform and azimuth arm are three-dimensional truss structures through which wind can flow. Wind can induce significant loads on this type of structure as it passes through several trusses that do not effectively shield one another.

To estimate the wind loads, we first applied two methods provided in the ASCE7-16[9] standard to calculate design wind loads on open structures (*Open Signs and Frames* for the first method, and *Trussed Towers* for the second method). Both methods rely on the structure's *solidity ratio*, which measures how open the structure is. First, the solidity ratio of the platform and azimuth arm are determined, as shown in Figure 9. Each method then provides an empirical formula to calculate an effective drag coefficient from the solidity ratio.

As a third method, we calculated the wind load assuming that the platform and azimuth arm were solid blocks with drag coefficients of 1.0.

All three methods require a dynamic wind pressure, calculated in Table 4 per the ASCE7-16 procedure. The wind load per the three methods is then calculated in Table 5.

Table 4: Calculation of dynamic wind pressure on platform and azimuth arm per ASCE7-16.

Quantity	Calculation or Assumption	Notes
Basic wind speed	V = 110 mph	Reference wind speed in this appendix.
Exposure category	B	
Terrain exposure constants	$\alpha = 7$ $z_g = 1{,}200$ ft	From exposure category.
Ground elevation factor	$K_e = 1.0$	Conservative. Neglects elevation above sea level.
Topographic factor	$K_{zt} = 1.0$	
Wind directionality factor	$K_d = 0.85$	Fixed value for *Open Signs and Frames* and *Trussed Towers* methods
Height above ground	z = 515 ft	Suspended structure average elevation above bottom of reflector
Velocity pressure coefficient	$K_z = 2.01\ (z/z_g)^{(2/\alpha)} = 1.58$	
Velocity pressure	$q_z = 0.00256\ K_z\ K_{zt}\ K_d\ K_e\ V^2 = 41.6$ psf	
Gust factor	G = 1.0	
Dynamic pressure	$q_z\ G = 41.6$ psf	

[9] American Society of Civil Engineers (ASCE). *ASCE 7-16. Minimum Design Loads and Associated Criteria for Buildings and Other Structures*. Chapters 26 and 29. 2016.

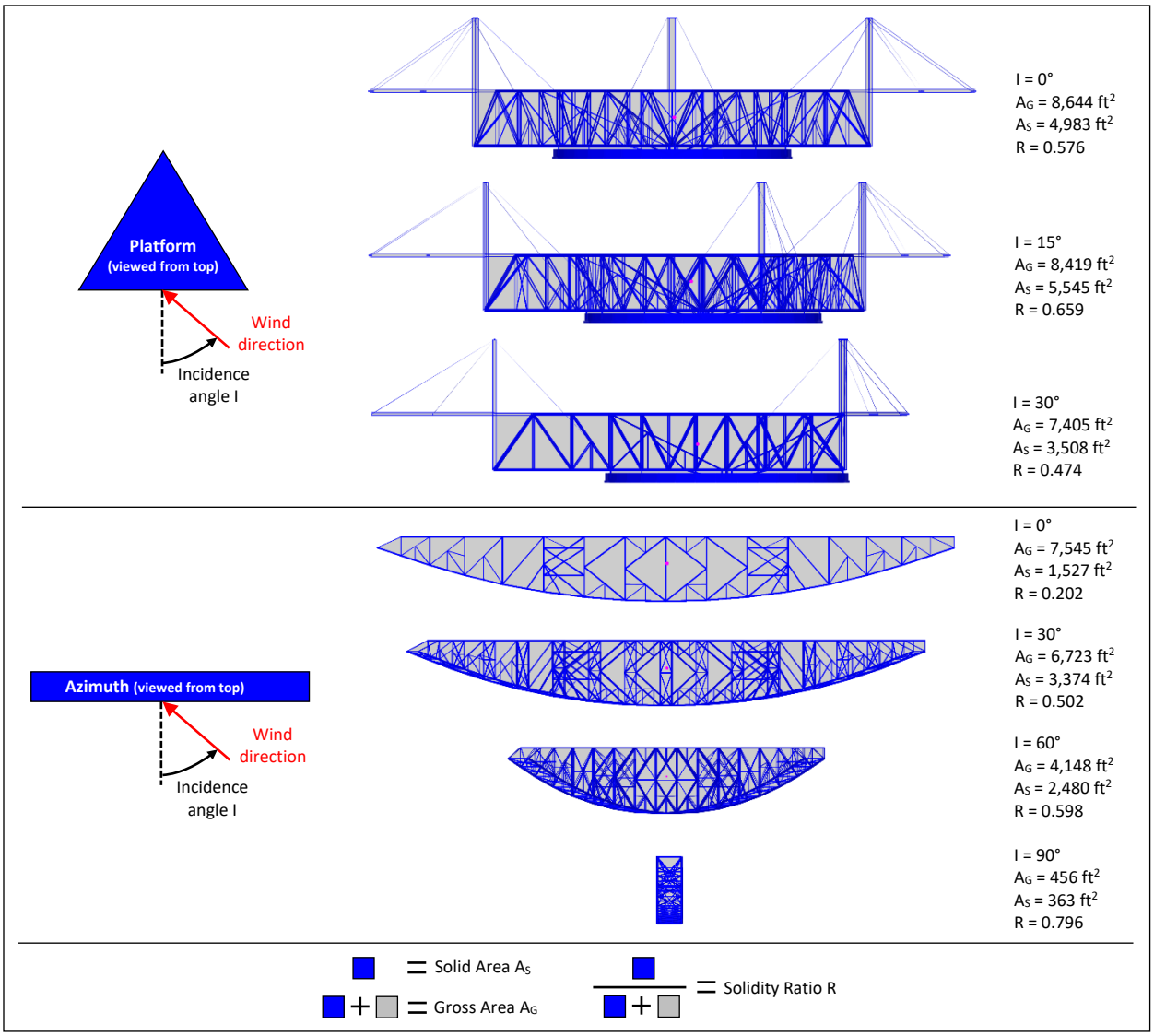

Figure 9: Platform and azimuth arm area properties for wind load calculation.

Table 5: Platform and azimuth arm wind load calculations at 110 mph (q_z G = 41.6 psf).

		Platform			Azimuth Arm			
Properties	**Incidence angle I [deg]**	0	15	30	0	30	60	90
	Gross area A_G [ft²]	8,644	8,419	7,405	7,545	6,723	4,148	456
	Solid area A_S [ft²]	4,983	5,545	3,508	1,527	3,374	2,480	363
	Solidity ratio R = A_S / A_G	0.576	0.659	0.474	0.202	0.502	0.598	0.796
ASCE7 *Open Signs and Frames* method	**Drag coeff.** $C = \begin{cases} 2.0 & R < 0.1 \\ 1.8 & 0.1 < R < 0.3 \\ 1.6 & R > 0.3 \end{cases}$	1.6	1.6	1.6	1.8	1.6	1.6	1.6
	Wind load F = q_z G C A_s [kip]	332	369	234	114	225	165	24
ASCE7 *Trussed Towers* method	**Drag coeff. C = 4 R² – 5.9 R + 4**	1.93	1.85	2.10	2.97	2.05	1.90	1.84
	Wind load F = q_z G C A_s [kip]	400	427	307	189	287	196	28
Solid drag method	**Drag coefficient C**	1.0	1.0	1.0	1.0	1.0	1.0	1.0
	Wind load F = q_z G C A_G [kip]	360	350	308	314	280	173	19

4.1.2 Gregorian

The wind load on the Gregorian is estimated through the simple drag force calculation shown in Table 6. Based on the hemispherical shape of the Gregorian dome, a drag coefficient of 0.5 is considered.

Table 6: Gregorian wind load calculation.

Quantity	Calculation or Assumption	Notes
Dynamic wind pressure	q_z G = 41.6 psf	Section 4.1.1 above.
Projected area	A = 3,850 ft^2	Approximately the same for all wind directions
Drag coefficient	C = 0.5	Drag coefficient for a sphere
Wind load	F = q_z G C A = 80 kip	

4.1.3 Total

The wind loads calculated above for the platform, azimuth arm, and Gregorian are combined in Figure 10 to obtain the total load on the suspended structure. The telescope is assumed to be in the stowed position, where the azimuth arm is 12 degrees off of the east-west direction. The total wind load is minimum when the wind is parallel to the azimuth arm. The three calculation methods result in total wind loads within 30 percent of each other for any wind direction.

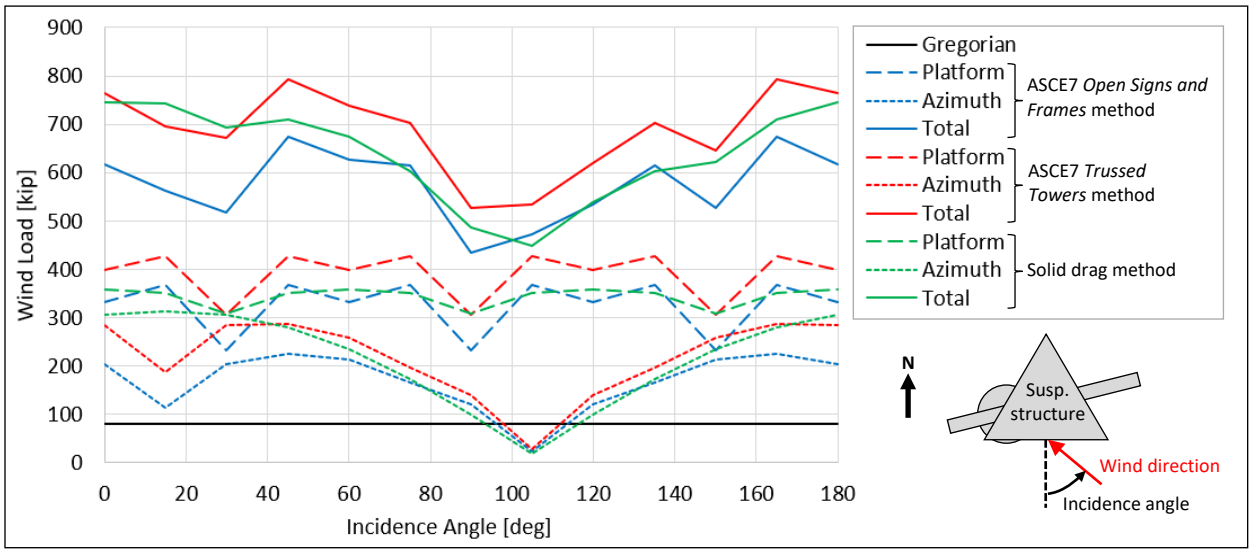

Figure 10: Calculated 110 mph wind load on suspended structure.

4.2 Towers

To estimate the wind load on the telescope's towers, we applied the method provided in ASCE7-16[10] to calculate design wind loads on *Chimneys, Tanks and Similar Structures*. This method is typically used for tall smokestacks, whose aspect ratios are comparable to the Arecibo towers.

The calculation and results are presented in Table 7 and Figure 11, where a different load is calculated for each tower segment based on the segment's width and average elevation. The dynamic wind pressure is calculated with similar parameters as for platform and azimuth arm (section 4.1.1 above): basic wind speed V = 110 mph, terrain exposure constants $\alpha = 7$ and z_g = 1,200 ft, topographic factor $K_{zt} = 1.0$, wind directionality factor $K_d = 0.9$ (fixed value for the *Chimneys, Tanks and Similar Structures* method), ground elevation factor $K_e = 1.0$ and gust-effect factor G = 1.0. In addition, for square cross-sections and tall aspect ratios, the method prescribes the force coefficient $C_f = 2.0$.

Table 7: 110 mph wind load calculation on towers.

		Tower 4 or 12				Tower 8					
Segment (1 = bottom, 4 or 6 = top)		**1**	**2**	**3**	**4**	**1**	**2**	**3**	**4**	**5**	**6**
Segment width	**w [ft]**	24	18	12	9	36	30	24	18	12	9
Segment height	**h [ft]**	63.4	63.4	63.4	63.4	61.4	61.4	61.4	61.4	61.4	61.4
Segment mid-elevation	**z [ft]**	407	470	533	597	291	352	414	475	536	598
Velocity pressure coefficient	**$K_z = 2.01\ (z/z_g)^{(2/\alpha)}$**	1.48	1.54	1.59	1.65	1.34	1.42	1.48	1.54	1.60	1.65
Velocity pressure	**$q_z = 0.00256\ K_z K_{zt} K_d K_e V^2$ [psf]**	41.1	42.9	44.4	45.9	37.4	39.5	41.3	43.0	44.5	45.9
Linear load	**$\lambda = q_z G C_f w$ [kip/ft]**	1.97	1.54	1.07	0.83	2.69	2.37	1.98	1.55	1.07	0.83
Segment load	**$F = \lambda h$ [kip]**	125	98	68	52	165	145	122	95	66	51
Tower load	**$\sum F$ [kip]**	343				644					

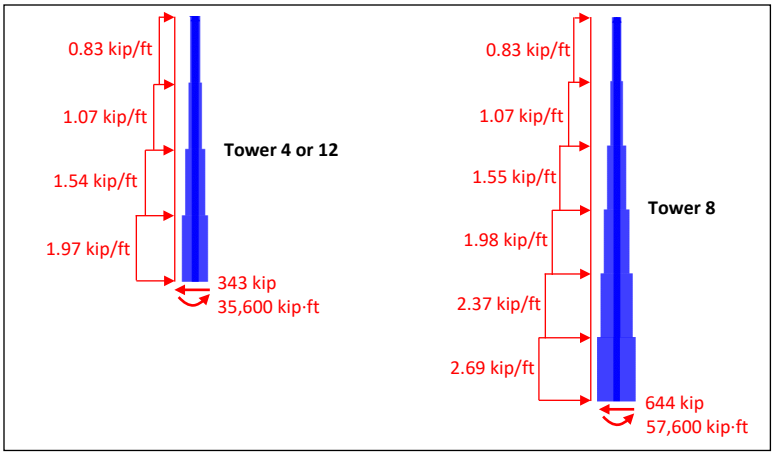

Figure 11: Calculated 110 mph wind load on towers.

[10] American Society of Civil Engineers (ASCE). *ASCE 7-16. Minimum Design Loads and Associated Criteria for Buildings and Other Structures*. Chapters 26 and 29. 2016.

4.3 Cables

The upgraded telescope structure included over four miles of main and backstay cables, which also caught wind. We estimated the wind load acting on the cables through the drag force calculation presented in Table 8. The calculation is simplified by assuming that the dynamic wind pressure at the elevation of the platform, calculated as q_z G = 41.6 psf per ASCE7-16[11] (section 4.1.1 above), applies to the entire length of each cable. The load is calculated for the case where the wind direction is perpendicular to the cable. The air flow is fully turbulent since the Reynolds number for a three-inch diameter cylinder perpendicular to a 110 mph wind is 250,000. In that regime, the drag coefficient of a cylinder can be taken as C = 1.2.

The total wind load on the cable system is shown in Figure 12 for different wind directions, considering the angle between the wind direction and each cable and assuming no shielding between parallel cables. The average total load on the main cables is 90 kip, half of which would be transferred to the suspended structure (45 kip). This is an order of magnitude less than the calculated wind load acting directly on the suspended structure (section 4.1.3 above).

Table 8: 110 mph wind load calculation on individual cables.

		Original	Original Backstays			Auxiliary	Auxiliary Backstays		
		Mains	Tower 4	Tower 8	Tower 12	Mains	Tower 4	Tower 8	Tower 12
Diameter	**D [in]**	3	3.25	3.25	3.25	3.25	3.625	3.625	3.625
Span	**S [ft]**	590	560	434	468	722	604	477	512
Linear Wind Load	**w = q_z G C D [lbf.ft^{-1}]**	12.5	13.5	13.5	13.5	13.5	15.1	15.1	15.1
Total Wind Load	**F = w S [kip]**	7.4	7.6	5.9	6.3	9.8	9.1	7.2	7.7
Linear Weight	**λ [lbf/ft]**	18.9	22.2	22.2	22.2	22.2	27.6	27.6	27.6
Wind-to-Weight Ratio	**w / λ**	0.66	0.61	0.61	0.61	0.61	0.55	0.55	0.55

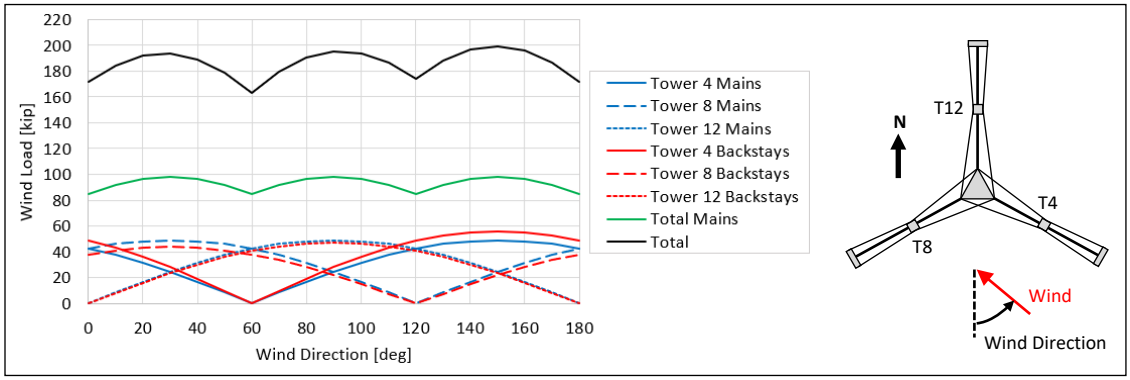

Figure 12: Calculated 110 mph wind load on cables.

The estimated wind load on a cable is of the same order of magnitude as the cable's weight, with ratios between 55 and 66 percent. The cable must therefore stretch and develop additional tension to carry this local wind load, in addition to any change of tension resulting from the global equilibrium of the structure. The cable tension increase

[11] American Society of Civil Engineers (ASCE). *ASCE 7-16. Minimum Design Loads and Associated Criteria for Buildings and Other Structures*. Chapters 26 and 29. 2016.

needed to carry the local wind load is calculated in Table 9. The wind load causes a horizontal deflection of up to 1.2 feet at midspan of the cable, but the corresponding tension increase is less than 0.3 percent of the pre-existing cable tension.

Table 9: Cable wind load effect on cable tensions.

		Original Main	Tower 4 Original Backstay	Auxiliary Main	Tower 4 Auxiliary Main
Length	**L [ft]**	589.877	560.024	721.538	603.972
Axial Rigidity	**EA [kip]**	135,587	158,657	155,638	198,115
Tension Before Wind	**T [kip]**	480.0	543.0	602.0	728.0
Linear Wind Load	**w [lbf/ft]**	12.5	13.5	13.5	15.1
Tension with Wind	**T' [kip]**	481.3	544.3	603.7	729.3
Length with Wind	$\mathbf{L' = \frac{2T'}{w} \sinh\left(\frac{wS}{2T'}\right)}$ **[ft]**	589.883	560.029	721.545	603.976
Check Tension and Length Compatibility	$\mathbf{T' = T + \frac{EA}{L}(L' - L)}$ **[kip]**	481.3 (matches)	544.3 (matches)	603.7 (matches)	729.3 (matches)
Relative Tension Increase due to Wind	$\mathbf{\frac{T' - T}{T}}$	0.27%	0.24%	0.28%	0.18%
Wind-Induced Horizontal Deflection [ft]	$\mathbf{S = \frac{T'}{w}\left(\cosh\left(\frac{wL}{2T'}\right) - 1\right)}$ **[ft]**	1.13	0.97	1.46	0.94

5.0 Computational Fluid Dynamic Analysis

As a second approach to determine the wind loads on the suspended platform, we performed a set of computational fluid dynamic (CFD) analyses. CFD has two benefits over the first-principle and standard design calculations presented above (section 4.0).

First, as a general numerical method, CFD applies to structures of any type and shape, including the telescope's unique suspended structure. By contrast, the standard design calculations use empirical formulas calibrated on typical structures. As a result, they may not be as accurate for unique structures like the telescope, although they can be adapted with conservative assumptions for design purpose as presented above. CFD is however expected to provide a more accurate estimate of the wind loads acting on the telescope's suspended structure.

Second, CFD captures the turbulence of the air flow passing through and around the suspended structure. Turbulence, which includes effects such as vortex shedding, can cause the wind load to fluctuate even when the wind speed is constant. Therefore, the magnitude and frequency of the load fluctuations need to be captured as they may cause vibration and resonance of the suspended structure during windstorms.

5.1 Similitude and Results Scaling

Each of the CFD analyses presented below applies a constant wind speed upstream of the suspended structure. The analysis is then run until the model reaches a quasi-steady state. Because of the turbulent airflow, the forces on the suspended structure may fluctuate with a fixed amplitude and frequency.

The results of a CFD analysis performed at a given wind speed can be scaled to another wind speed, as long as the airflow is fully turbulent for both speeds. The equations relevant to the scaling process are provided in Table 10. First, an airflow is considered fully turbulent if its Reynolds number is greater than 100,000. Then, as long as the airflow remains fully turbulent, the wind pressure is proportional to the square of the wind speed, and the

turbulence frequency is proportional to the ratio of the wind speed to the characteristic length. This scaling method is commonly applied to wind tunnel test results to determine the loads due to wind speeds that are too high to be practically achieved in a wind tunnel.

Table 10: Flow similitude and scaling.

	Flow #1 (wind tunnel or CFD)	Flow #2 (actual)
Characteristic Length	L_1	L_2
Fluid Kinematic Velocity	v_1	v_2
Wind Velocity	U_1	U_2
Reynolds Number	$\mathrm{Re}_1 = \frac{U_1 L_1}{v_1}$	$\mathrm{Re}_2 = \frac{U_2 L_2}{v_2}$
Wind Pressure (scaling also applicable to resultant forces and moments)	p_1	$p_2 = p_1 \left(\frac{U_2}{U_1}\right)^2$ if $\mathrm{Re}_1 > 10^5$ and $\mathrm{Re}_2 > 10^5$
Wind Turbulence Frequency	f_1	$f_2 = f_1 \left(\frac{U_2 L_1}{U_1 L_2}\right)$ if $\mathrm{Re}_1 > 10^5$ and $\mathrm{Re}_2 > 10^5$

5.2 CFD Model

We performed the CFD analyses with the PaceFish solver. PaceFish implements a Lattice Boltzmann Method (LBM) on a cartesian structured mesh, and runs analysis on Graphical Processing Units (GPUs) through a cloud service.

The objective of the CFD analysis is to determine the wind loads on the suspended structure. Therefore, as shown in Figure 13, the model does not include the towers and cables. The suspended structure is assumed fixed and rigid and is placed in a computational domain through which the air flow is simulated. Each truss member of the platform and azimuth arm is modeled, in addition to the ring girder and Gregorian dome. However, smaller features such as member lacing, connection plates, or outrigger cables are omitted. These features are too small to be realized within the mesh of the computational domain, which was made just fine enough to provide accurate results for the overall wind load. The suspended structure is modeled with the azimuth arm and Gregorian in the stowed position, as they were during significant windstorms.

Each analysis applies a constant wind speed upstream of the suspended structure. However, the Lattice Boltzmann Method is transient, and therefore each analysis is run until a quasi-steady state is achieved. In that state, the pressures and forces of the structure are either constant or fluctuating with a constant amplitude and frequency due to turbulence. The turbulence model is an Improved Delayed Detached Eddy Simulation (IDDES kw-SST).

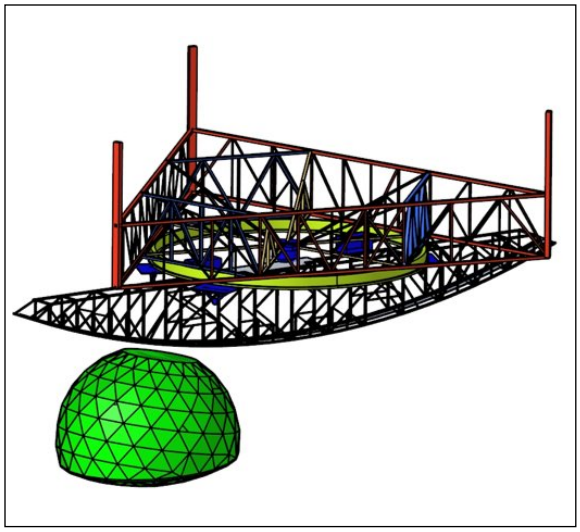

Figure 13: Suspended structure geometry in CFD model.

With the structure modeled at full scale, the CFD analyses are performed at 22.4 mph (10 meter per second, or m/s) wind speed. As shown in Table 11, this wind speed is sufficiently high for the flow to be fully turbulent around the smaller elements of the suspended structure. The results obtained from the CFD analyses at 22.4 mph can therefore be scaled to the actual maximum wind speed of 110 mph (section 5.1 above). Like for an actual wind tunnel test, running the CFD analysis at a lower wind speed is more practical. In addition, a larger mesh size can be used in the computational domain, which can make the analysis orders of magnitude faster to complete.

Table 11: Reynolds numbers of CFD and actual flows on suspended structure (air kinematic viscosity v = 1.61 10^{-4} ft^2/s).

		Platform		Gregorian		Steel Member	
		CFD Model	**Actual**	**CFD Model**	**Actual**	**CFD Model**	**Actual**
Characteristic Length	**L [ft]**	216	216	84	84	1	1
	[mph]	22.4	110	22.4	110	22.4	110
Wind Speed	**U [m/s]**	10	49	10	49	10	49
	[ft/s]	33	161	33	161	33	161
Reynolds Number	$\mathbf{Re = \frac{UL}{v}}$	4.4 10^7	2.2 10^8	1.7 10^7	8.4 10^7	2.0 10^5	1.0 10^6
Fully-Turbulent?	**Re > 10^5?**	yes	yes	yes	yes	yes	yes

5.3 Results

In two separate CFD analyses, a wind speed of 22.4 mph (10 m/s) was applied in two orthogonal directions: north wind (wind blows from north to south) and west wind (west to east).

In each analysis, the CFD solver determines the pressure on the model's surfaces. The pressure is then integrated over the model to obtain the resultant wind loads acting on the structure, which are forces and moments in three directions. Separate integrations are performed for the platform, azimuth arm, and Gregorian to determine the loads on each substructure, as defined in Figure 16. The loads are time-dependent since the analysis is transient. However, they eventually reach a quasi-steady state where each load is either essentially constant, or fluctuates with fixed amplitude and frequency. The air velocity in different planes cutting through the suspended structure is shown in Figure 14 and Figure 15.

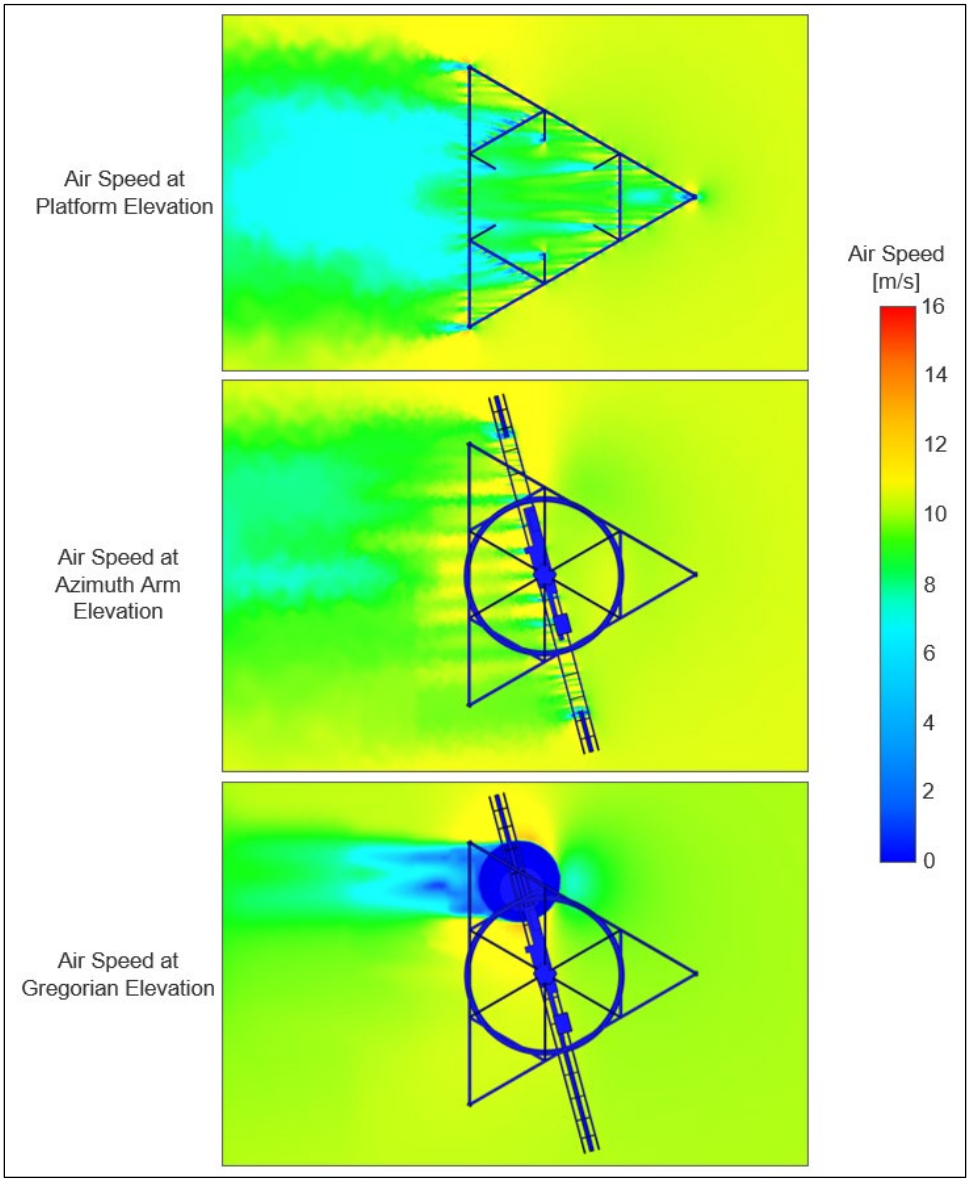

Figure 14: Air velocity around suspended structure in CFD analysis of 22.4 mph (10 m/s) north wind.

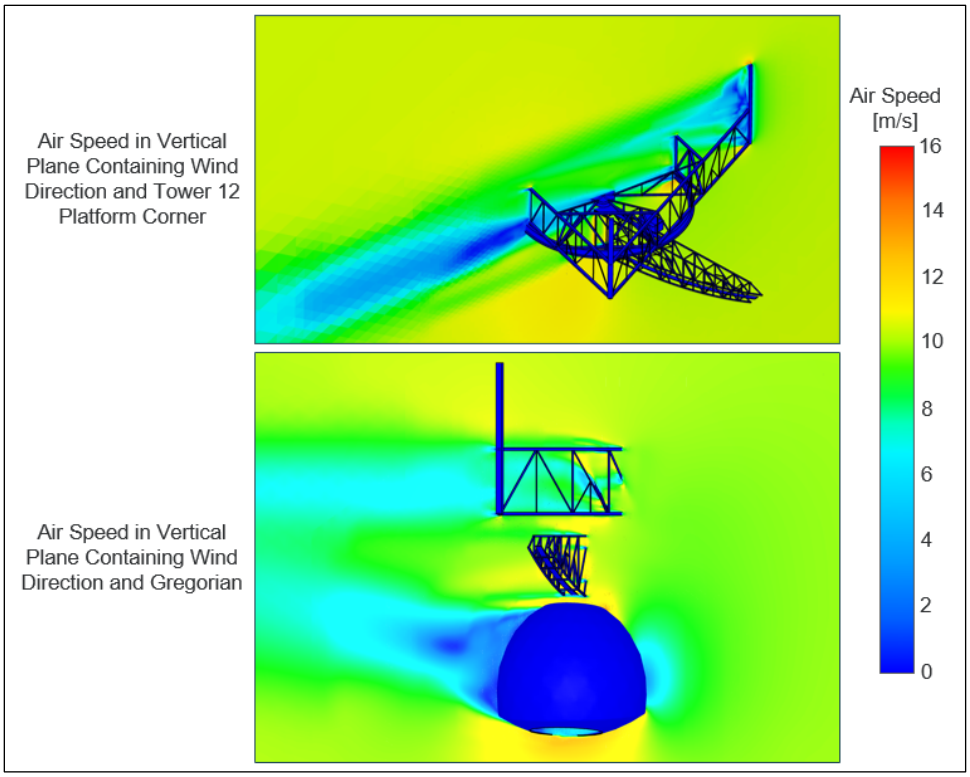

Figure 15: Air velocity around suspended structure in CFD analysis of 22.4 mph (10 m/s) north wind.

The loads on the platform, azimuth arm and Gregorian for 60 seconds of quasi-steady state are shown in Figure 17 (north wind) and Figure 18 (west wind). The average value and the amplitude and frequency of the fluctuation (turbulence) of the loads are summarized in Table 12 (north wind) and Table 13 (west wind). The tables provide these results as retrieved from the CFD model with a 22.4 mph wind and after scaling to the reference wind speed on 110 mph (section 5.1 above). The most significant wind forces are also summarized in Figure 19.

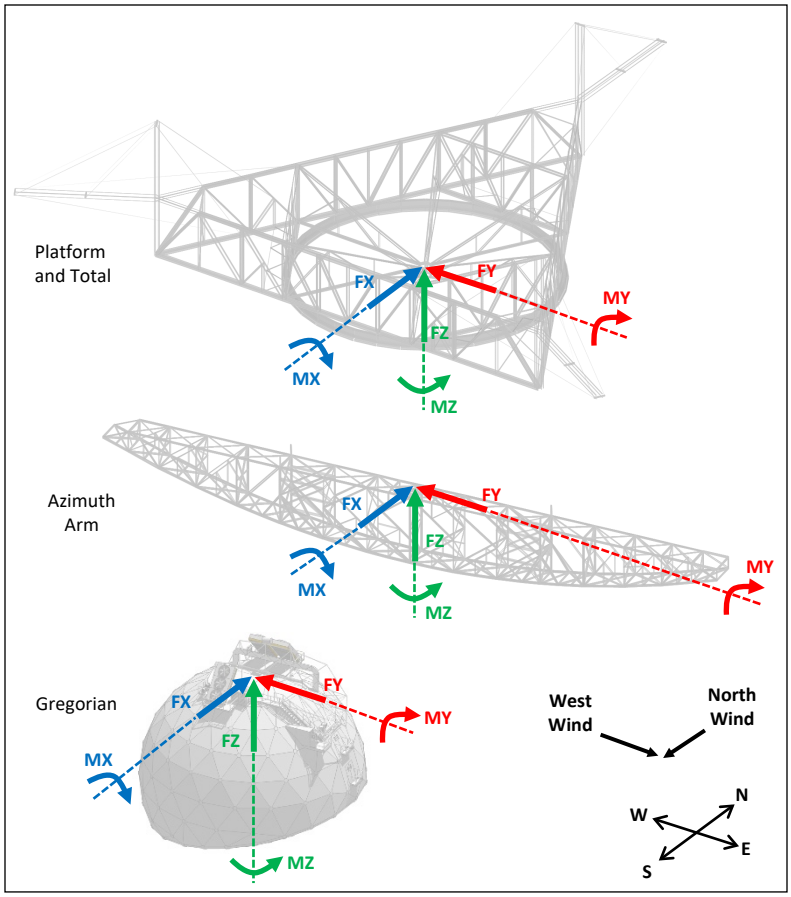

Figure 16: Resultant forces and moments on platform, azimuth arm and Gregorian.

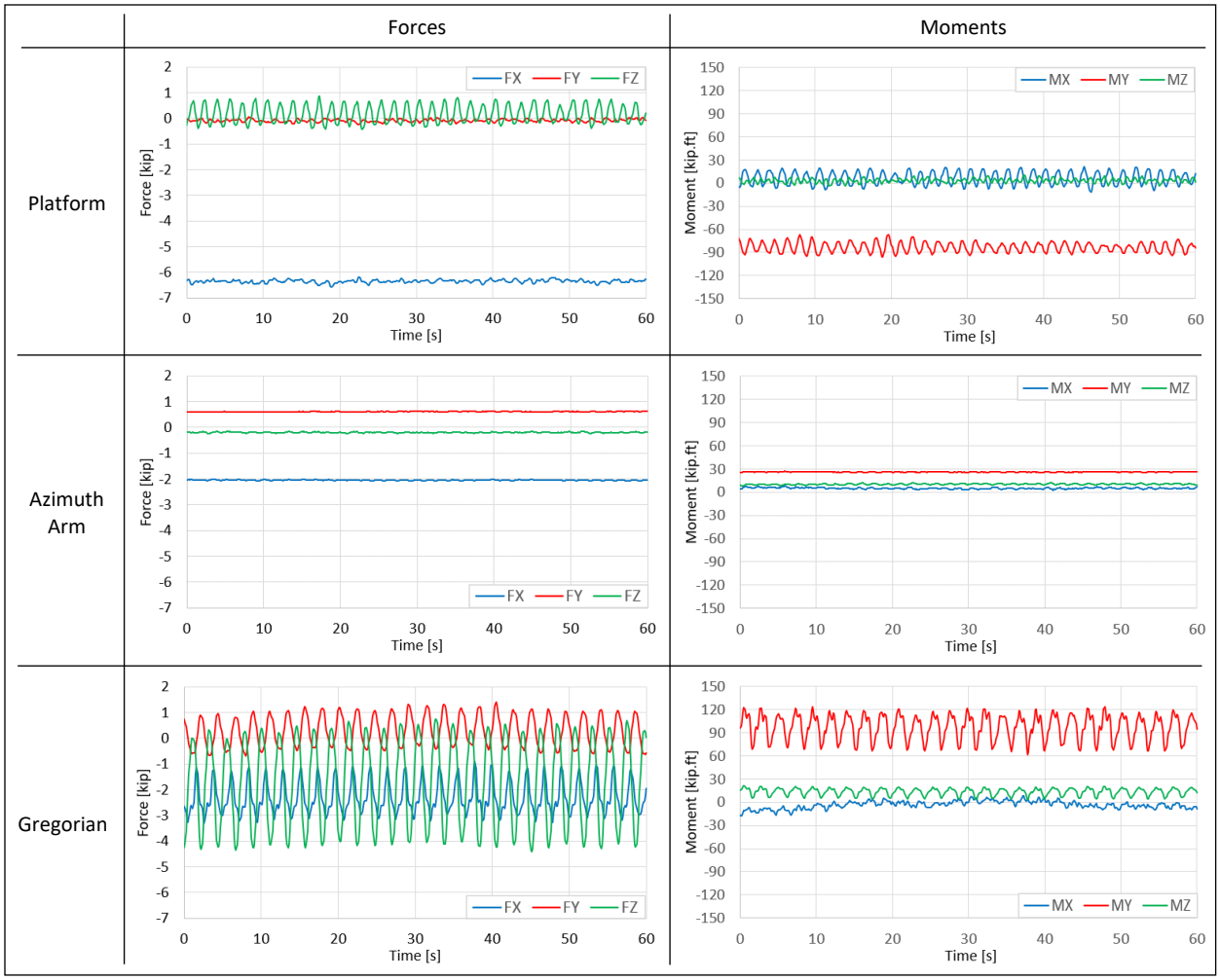

Figure 17: Resultant forces and moments on suspended structure in quasi-steady state for 22.4 mph (10 m/s) north wind.

Table 12: Resultant forces and moments on suspended structure in quasi-steady state for north wind.

		CFD Results (22.4 mph)						Scaled to Reference Wind Speed (110 mph)					
		Average		Turbulence Amplitude		Turbulence Frequency		Average		Turbulence Amplitude		Turbulence Frequency	
		F [kip]	M [kip·ft]	F [kip]	M [kip·ft]	f_F [Hz]	f_M [Hz]	F [kip]	M [kip·ft]	F [kip]	M [kip·ft]	f_F [Hz]	f_M [Hz]
Platform	**X**	-6.4	7.5		12.5		0.61	-155	181		302		3.00
	Y	-0.1	-82.5		7.5		0.61	-2	-1,995		181		3.00
	Z	0.2	5.0	0.5		0.61		5	121	12		3.00	
Azimuth Arm	**X**	-2.0	5.0					-48	121				
	Y	0.6	26.0					15	629				
	Z	-0.2	10.0					-5	242				
Gregorian	**X**	-2.2	-5.0	1.0		0.44		-53	-121	24		2.19	
	Y	0.2	90.0	0.8	25.0	0.44	0.44	5	2,176	19	605	2.19	2.19
	Z	-1.9	12.5	2.3	7.5	0.44	0.44	-46	302	56	181	2.19	2.19
Total	**X**	-10.6	-68.0	1.0	164.8			-256	-1,644	24	3,986		
	Y	0.7	150.9	0.8	64.0			17	3,648	19	1,549		
	Z	-1.9	132.3	2.8	62.8			-46	3,200	68	1,518		

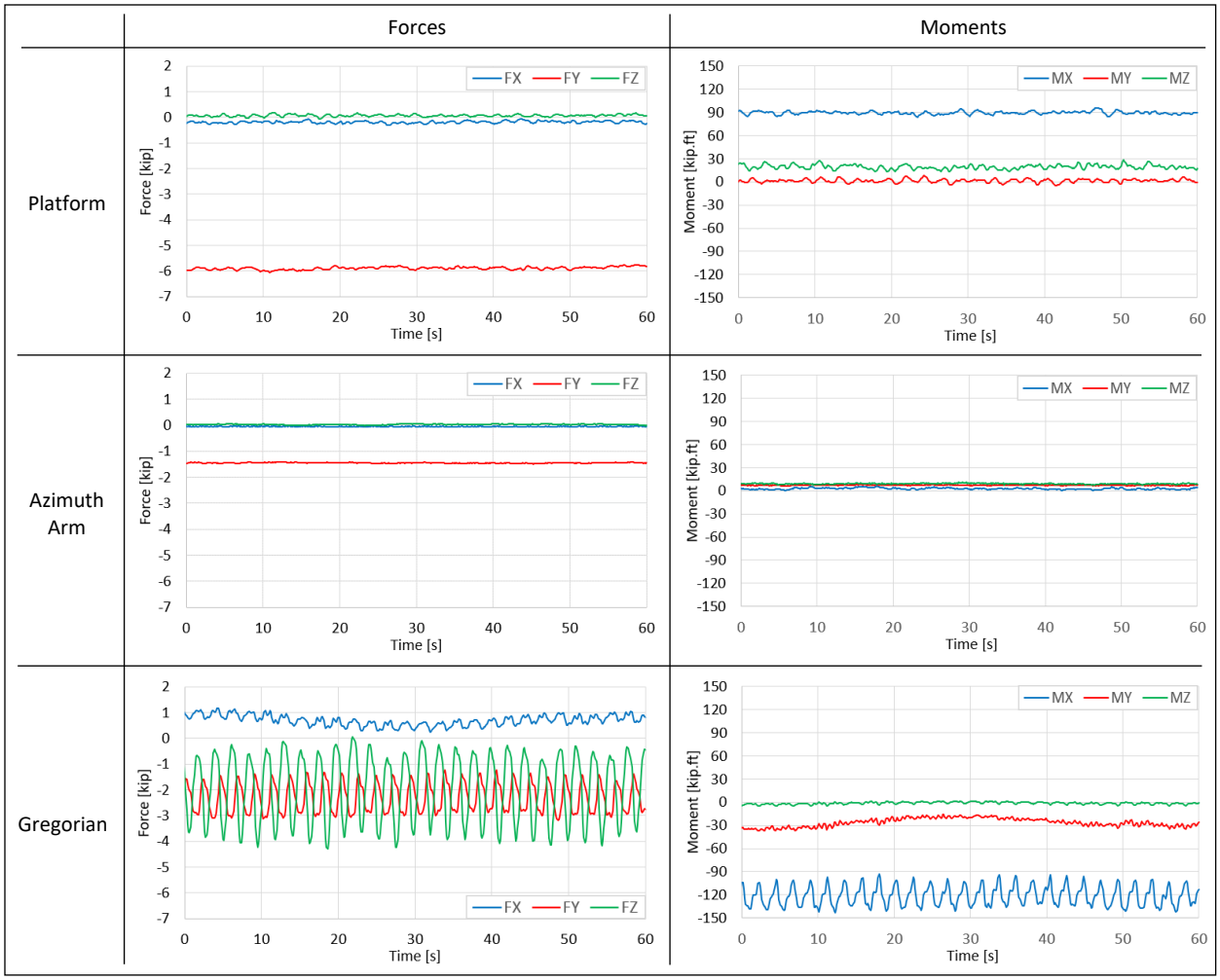

Figure 18: Resultant forces and moments on suspended structure in quasi-steady state for 22.4 mph (10 m/s) west wind.

Table 13: Resultant forces and moments on suspended structure in quasi-steady state for west wind.

		CFD Results (22.4 mph)						Scaled to Reference Wind Speed (110 mph)					
		Average		Turbulence Amplitude		Turbulence Frequency		Average		Turbulence Amplitude		Turbulence Frequency	
		F [kip]	M [kip·ft]	F [kip]	M [kip·ft]	f_F [Hz]	f_M [Hz]	F [kip]	M [kip·ft]	F [kip]	M [kip·ft]	f_F [Hz]	f_M [Hz]
Platform	**X**	-0.2	90.0					-5	2,176				
	Y	-5.9	20.0					-143	484				
	Z	0.1	0.0					2	0				
Azimuth Arm	**X**	-0.1	3.0					-2	73				
	Y	-1.5	7.0					-36	169				
	Z	0.0	9.0					0	218				
Gregorian	**X**	0.8	-120.0	0.2	20.0	0.44	0.44	19	-2,902	5	484	2.19	2.19
	Y	-2.3	-30.0	0.8		0.44		-54	-725	19		2.19	
	Z	-2.2	-2.0	1.7		0.44		-53	-48	41		2.19	
Total	**X**	0.5	-267.0	0.2	143.3			12	-6,457	5	3,465		
	Y	-9.7	-61.7	0.8	4.3			-235	-1,492	19	104		
	Z	-2.1	-12.1	1.7	16.5			-51	-293	41	399		

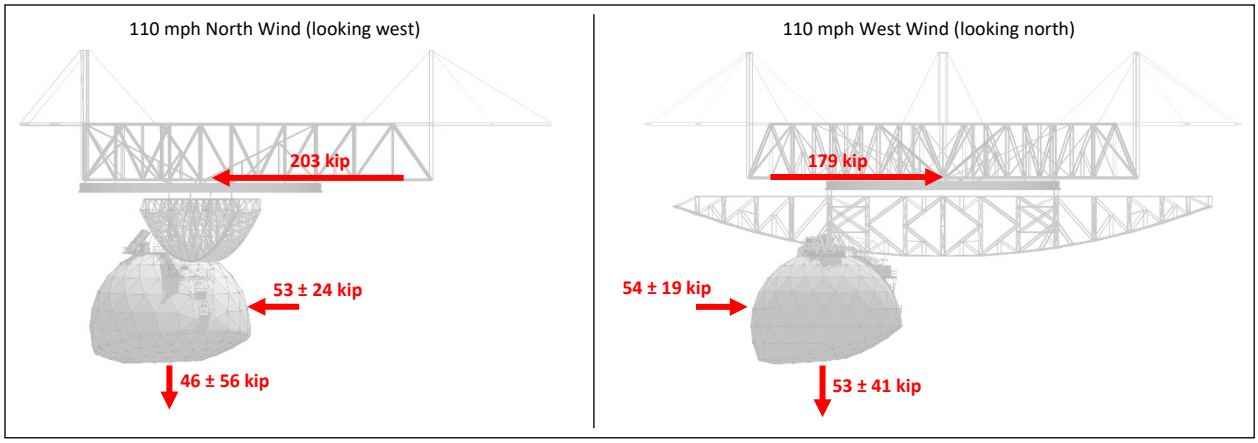

Figure 19: Main wind forces on suspended structure.

5.4 Validation

As a first validation of the CFD model, we compared the results of CFD analysis to the results of the wind tunnel study performed in 1993 (section 2.3 above). The comparison is limited to the loads on the Gregorian since the wind tunnel study does not provide the loads on the platform and azimuth arm. Nevertheless, the wind tunnel tests were performed on a full model of the suspended structure like in the CFD analyses, and therefore the results for the Gregorian are comparable. The comparison is shown in Figure 20. The two sets of wind loads are generally consistent, considering that some of the wind tunnel test parameters are unknown and may differ from the CFD analyses.

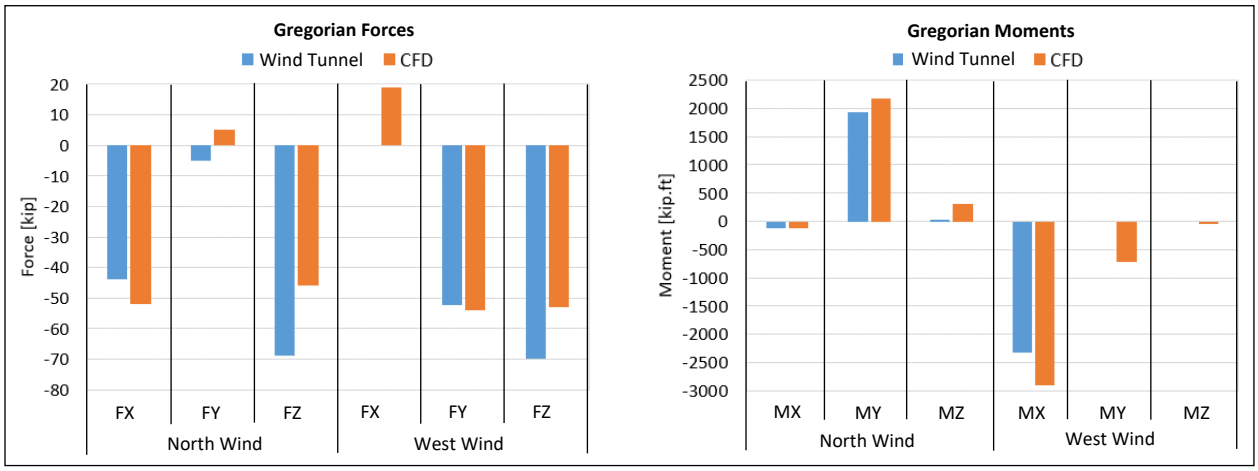

Figure 20: Comparison of Gregorian forces and moments from wind tunnel test and CFD analysis at 110 mph.

To verify that the CFD results can be scaled to higher wind speeds, we repeated the north wind analysis with the speed doubled to 44.8 mph (20 m/s) and compared the results with the original analysis at 22.4 mph (10 m/s). The comparison is shown in Figure 21 and Table 14 for the forces acting on the platform as an example. We observe that when the wind speed doubles, the average force and turbulence amplitude essentially quadruple, while the turbulence frequency essentially doubles. The same ratios were observed for the forces and moments on the platform, azimuth arm, and Gregorian. The behavior of the CFD model is therefore as expected and confirms that the flow is fully turbulent, such that the CFD results can be scaled instead of running the CFD model for more wind speeds.

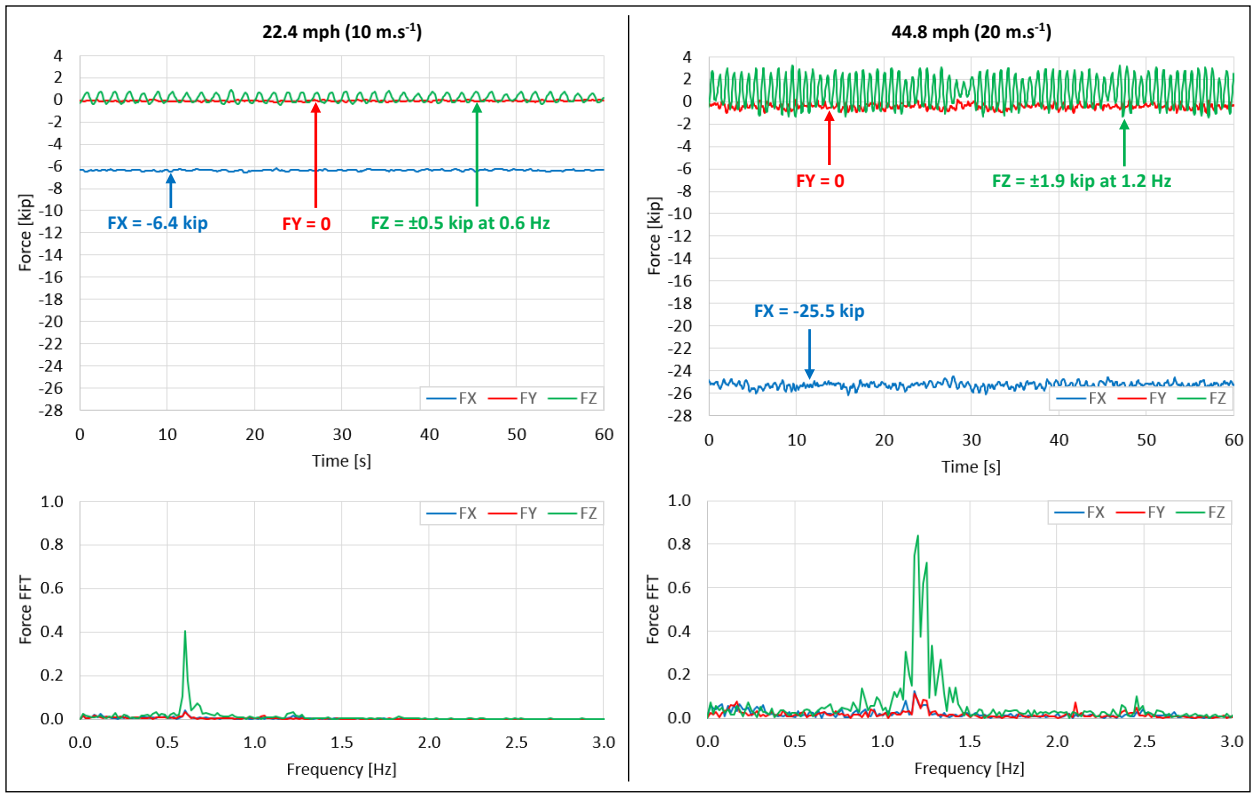

Figure 21: Resultant forces on platform in quasi-steady state for 22.4 mph (10 m/s) and 44.8 (20 m/s) north wind.

Table 14: Difference in resultant forces on platform between quasi-steady state for 22.4 mph (10 m/s) and 44.8 mph (20 m/s) north wind.

	FX Average [kip]	FZ Amplitude [kip]	FZ Frequency [Hz]
22.4 mph	-6.4	0.5	0.6
44.8 mph	-25.5	1.9	1.2
Ratio (44.8 mph) / (22.4 mph)	4.0	3.8	2.0

6.0 Dynamic Structural Response Analysis

We performed a series of dynamic analyses on the finite element (FE) models of the original and upgraded telescope to determine the structure's response to wind loads. This section describes the set-up of the analyses, which includes the construction of time-dependent wind loads from the CFD results, their application to the FE models, and the selection of simulated wind conditions. The results of the analyses are presented in section 0 below. The FE models of the telescope are described in Appendix F.

6.1 Wind Conditions and Directions

We analyzed the behavior of the telescope in two wind conditions: ambient wind and Hurricane Maria. For each condition, we extracted a 2.5-hour segment of the wind speed data recorded at one-second intervals on the telescope's platform (Figure 22).

The **ambient wind** speed was recorded at daytime on July 15, 2019 and is representative of the wind speed experienced on most summer days at the Observatory.

For **Hurricane Maria**, we combined the wind speed data recorded by two instruments: an anemometer, which recorded the instantaneous wind speed at one-second intervals but failed approximately one hour before the peak of the storm, and a doppler, which recorded the instantaneous wind speed at 15-second intervals for the entire duration of the storm (Section 3.1). The doppler data cannot be used directly in a dynamic analysis of the telescope because the 15-second interval is larger than the natural period of the structure. However, the doppler data captures the peak intensity of the storm, and we used it to scale the anemometer data to that peak intensity. The maximum 10-minute average speed is 69 mph and 50 mph in the doppler and anemometer data respectively. We therefore added the difference of 19 mph to the anemometer data, such that its maximum 10-minute average matches the actual maximum of 69 mph captured by the doppler. Every 10 minutes, the doppler also logged the peak instantaneous wind speed over the past 10 minutes (Section 3.1), and the maximum during Hurricane Maria is 108 mph. The scaled anemometer data has a peak instantaneous wind speed of 118 mph, and using it in the analysis is therefore slightly conservative.

For both wind conditions, we considered three wind directions corresponding the three tower-to-platform directions (Figure 23). For each wind direction, the load on the platform is most effectively resisted by the main cables connected to one of the towers, which maximizes the tension increase in those cables. Cable tension results will be reported as envelopes over the three wind directions for each wind condition.

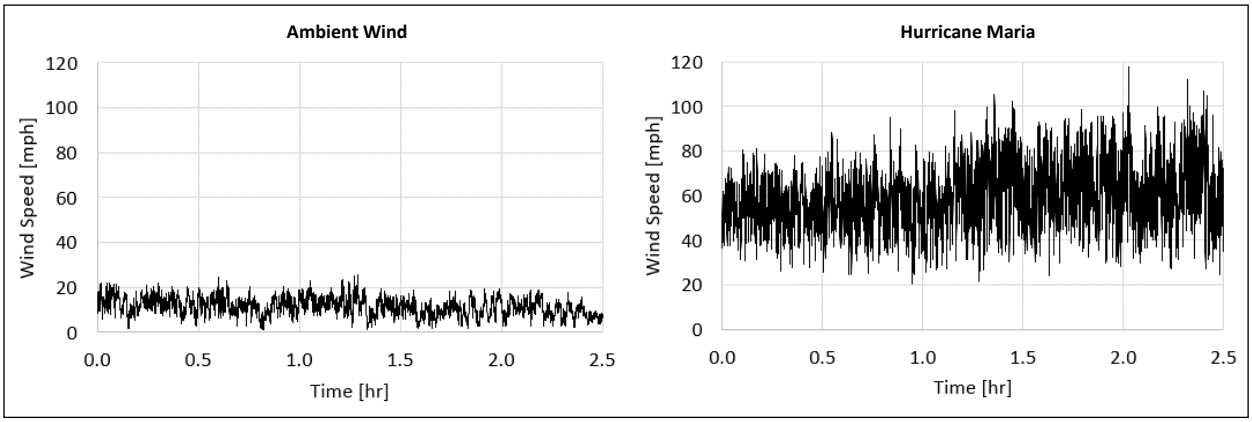

Figure 22: Wind speed time histories considered.

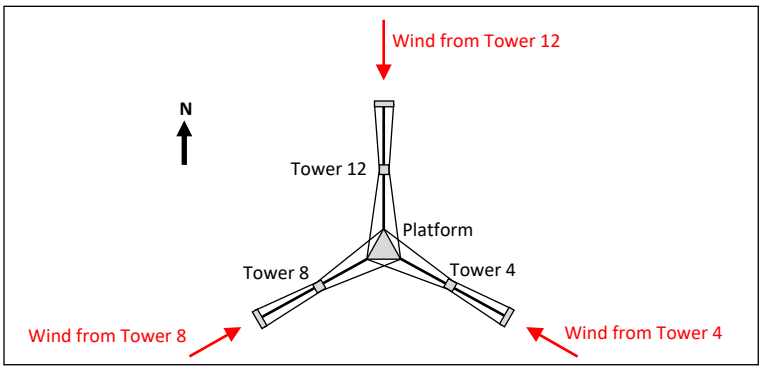

Figure 23: Wind directions considered.

6.2 Time-dependent Wind Loads

6.2.1 Suspended Structure

If the wind speed was constant, each wind load (force and moment on platform, azimuth arm, and Gregorian) could be idealized as a periodic load with three parameters: mean value, turbulence amplitude, and turbulence frequency. As described in Section 0, we determined these parameters through computational fluid dynamic (CFD) analysis for a constant wind speed of 22.4 mph (10 m/s).

The parameters of the periodic load induced by a constant wind speed on a given object are tied to the wind speed as follows: the turbulence frequency is directly proportional to the speed, while the mean value and turbulence amplitude are proportional to the square of the speed. To approximate the load induced by a time-varying wind speed, we considered a sinusoid function and varied its parameters over time based on the wind speed. This process is described in Table 15 and Figure 24.

Examples of wind load time histories on the platform, azimuth arm and Gregorian constructed from CFD results and wind speed time history are provided in Figure 25.

Table 15: Construction of wind load time history from CFD results and wind speed time history.

CFD Wind Speed	U_{CFD}
CFD Mean Load	$P_{CFD,mean}$
CFD Turbulence Amplitude	$P_{CFD,turb}$
CFD Turbulence Frequency	f_{CFD}
CFD Load Time History	$P_{CFD}(t) = P_{CFD,mean} + P_{CFD,turb}\sin(2\pi f_{CFD}t)$
Actual Velocity Time History	$U(t)$
Actual Turbulence Frequency	$f(t) = f_{CFD}\left(\frac{U(t)}{U_{CFD}}\right)$
Load Time Step	dt
Actual Turbulence Phase	$\phi(0) = 0$ $\phi(t) = \phi(t - dt) + 2\pi f(t)dt$
Actual Load Time History	$P(t) = \left(P_{CFD,mean} + P_{CFD,turb}\sin(\phi(t))\right)\left(\frac{U(t)}{U_{CFD}}\right)^2$

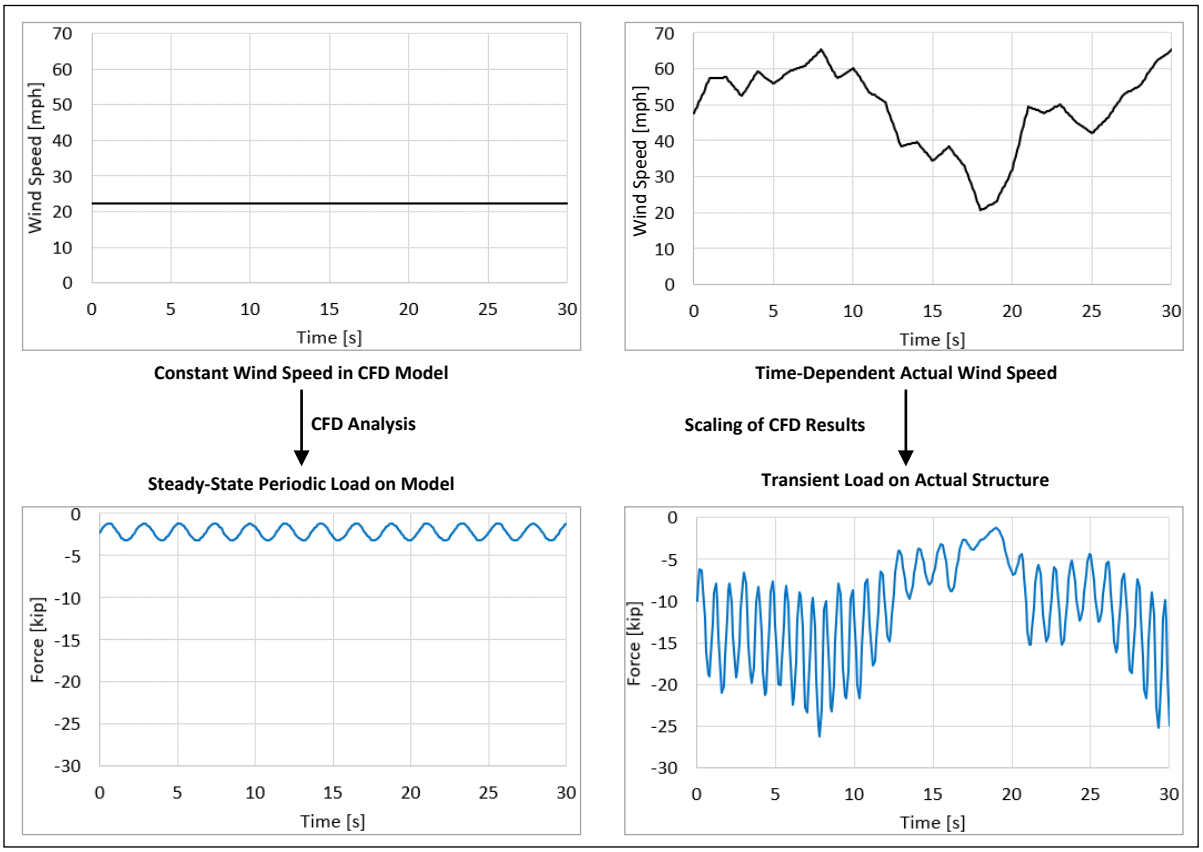

Figure 24: Construction of wind load time history from CFD results and wind speed time history.

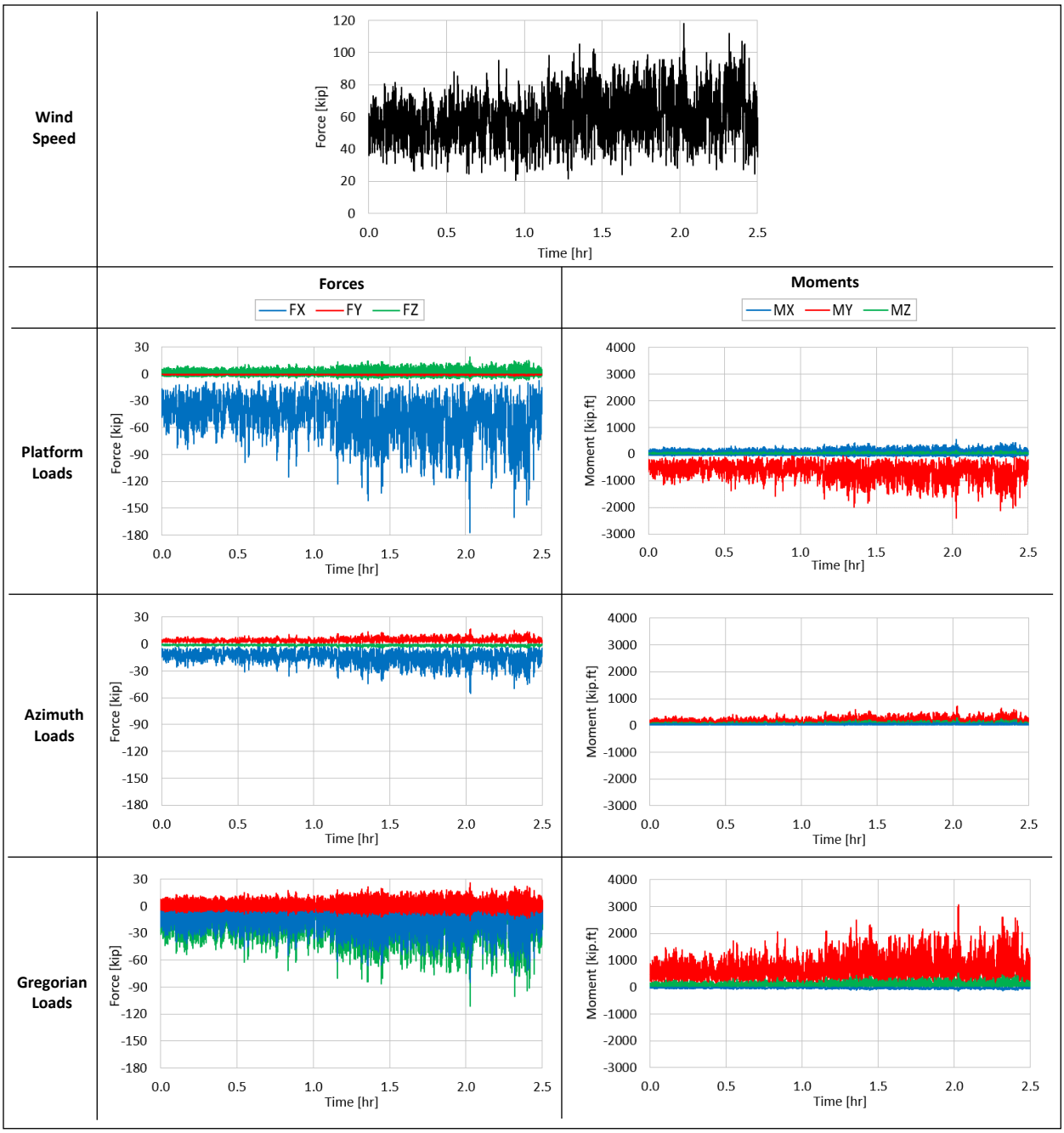

Figure 25: Wind loads on suspended structure under hurricane wind from Tower 12 (north-south).

6.2.2 Towers

For the three towers, we constructed the wind load time histories by scaling the calculated static wind loads (section 4.2 above) with the square of the wind speed. Examples of resulting wind load time histories are provided Figure 26.

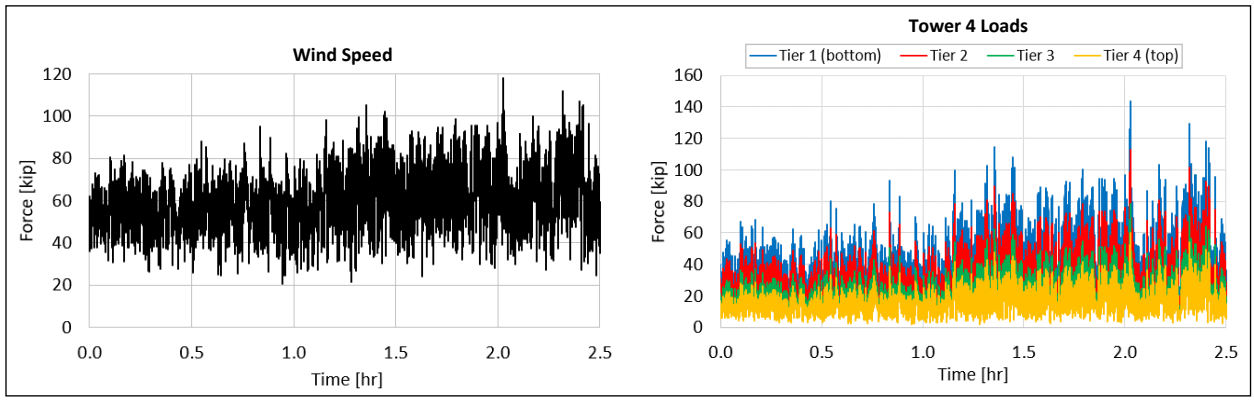

Figure 26: Wind loads on Tower 4 under hurricane wind from Tower 12.

6.3 Load Application

In the FE models, the wind loads are applied to the suspended structure as shown in Figure 27. For the platform and azimuth arm, multiple nodes are loaded to obtain the desired resultant force or moment. For the Gregorian, which is not modeled as elements, the resultant forces and moments are applied at the bottom of the azimuth arm where the Gregorian is located when the telescope is stowed. Finally, the wind loads on the towers are applied as line loads.

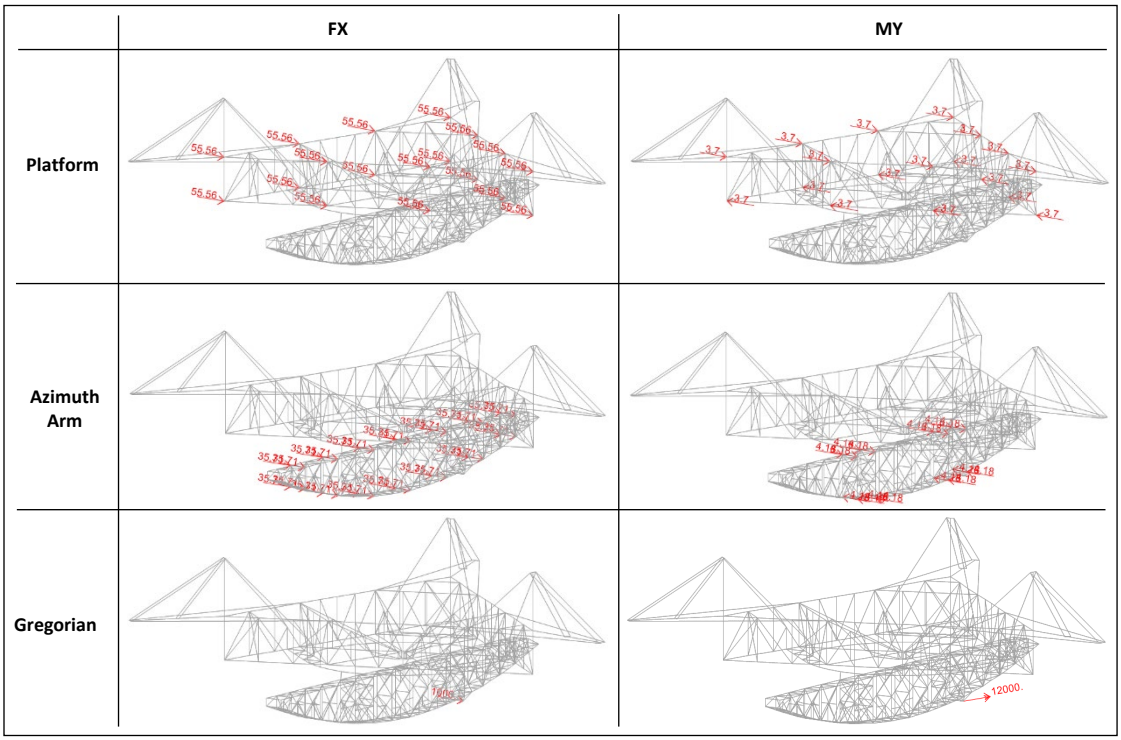

Figure 27: Examples of load application to suspended structure.

6.4 Wind Analyses Performed

As shown in Table 16, we performed total of 12 analyses considering two structures (original and upgraded), two wind conditions (ambient and Hurricane Maria) and three wind directions (from each of the three towers toward the platform). While the original structure (1964-1997) did not experience Hurricane Maria (2017), this storm is a conservative event to evaluate the potential impact of past hurricanes on the original structure. The tiedowns of the upgraded structure were released in the analysis of Hurricane Maria, consistently with the Observatory's practice of releasing the tiedowns before significant storms. Each analysis is a linear dynamic analysis simulating 2.5 hours of wind and solved through modal superposition, with a damping ratio of one percent on each mode.

Table 16: Wind analyses performed.

Analysis #	Structure	Tiedowns	Wind Condition	Wind Direction
1	Original	Taut	Ambient wind	Tower 4 → Platform
2	Original	Taut	Ambient wind	Tower 8 → Platform
3	Original	Taut	Ambient wind	Tower 12 → Platform
4	Original	Taut	Hurricane Maria	Tower 4 → Platform
5	Original	Taut	Hurricane Maria	Tower 8 → Platform
6	Original	Taut	Hurricane Maria	Tower 12 → Platform
7	Upgraded	Taut	Ambient wind	Tower 4 → Platform
8	Upgraded	Taut	Ambient wind	Tower 8 → Platform
9	Upgraded	Taut	Ambient wind	Tower 12 → Platform
10	Upgraded	Slack	Hurricane Maria	Tower 4 → Platform
11	Upgraded	Slack	Hurricane Maria	Tower 8 → Platform
12	Upgraded	Slack	Hurricane Maria	Tower 12 → Platform

7.0 Cable Tension Results

7.1 Original Structure

The cable tension time histories in the original structure are shown in Figure 28 for one wind direction of the ambient and hurricane conditions. For the ambient condition, the fluctuations of the cable tensions are minimal compared to the pre-existing tensions. The rest of the results presented in this section are therefore focused on the hurricane condition. The cable tension maps (Figure 29, Figure 30 and Figure 31) show the envelope of the hurricane results for the three wind directions considered.

Figure 29 shows the maximum tension increase in each cable during the hurricane as a percentage of the pre-hurricane tension. Excluding the tiedowns, the maximum tension increase is nine percent and occurs in the backstays of tower 8.

Figure 30 shows the lowest safety factor reached in each cable during the hurricane. The lowest safety factor is the ratio of the highest cable tension experienced during the hurricane to the cable's minimum breaking strength. The safety factors remain around two in all of the cables.

Figure 31 shows the maximum normalized stress range experienced by each cable during the hurricane. The maximum normalized stress range is the ratio of the maximum tension range (difference between maximum and minimum tension experienced) to the cable's minimum breaking strength. The maximum normalized stress range is between three and five percent in the mains and backstays.

Table 17 indicates the number of stress cycles experienced by each cable per hour of hurricane wind condition, for different stress levels. The number of cycles were counted in the cable tension time history results using the rainflow method, and averaged over the three wind directions considered.

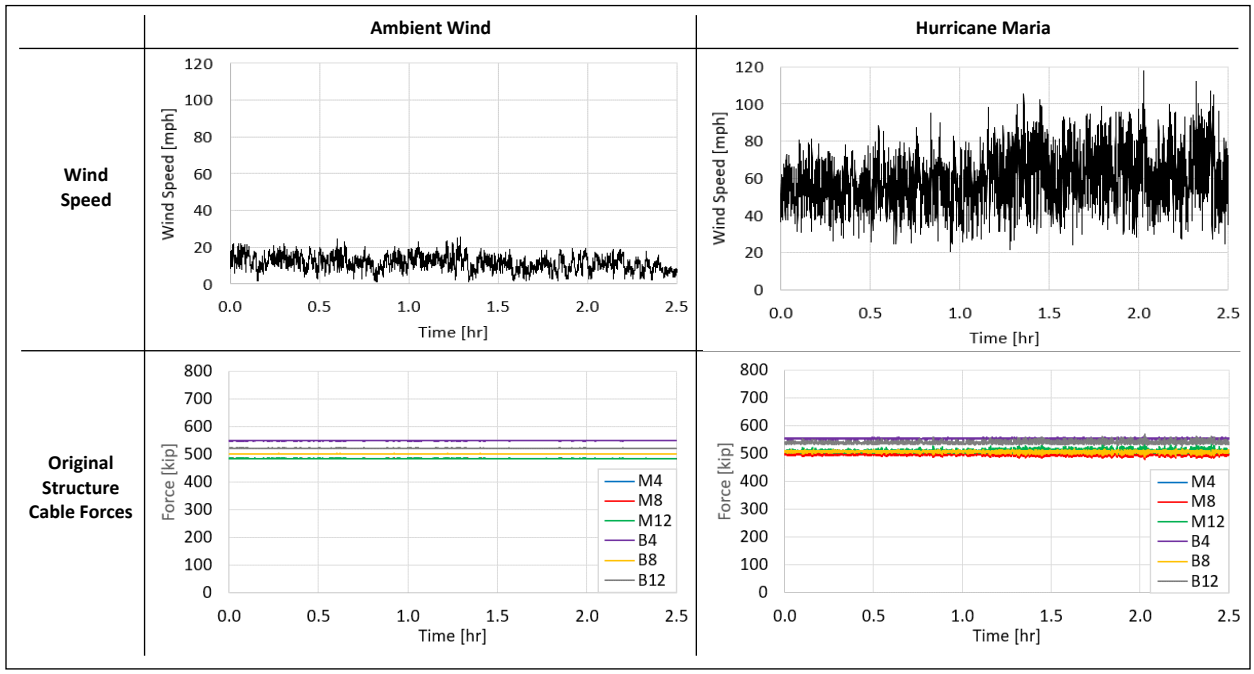

Figure 28: Cable tension time history in original structure under ambient and hurricane wind from Tower 12 (north-south).

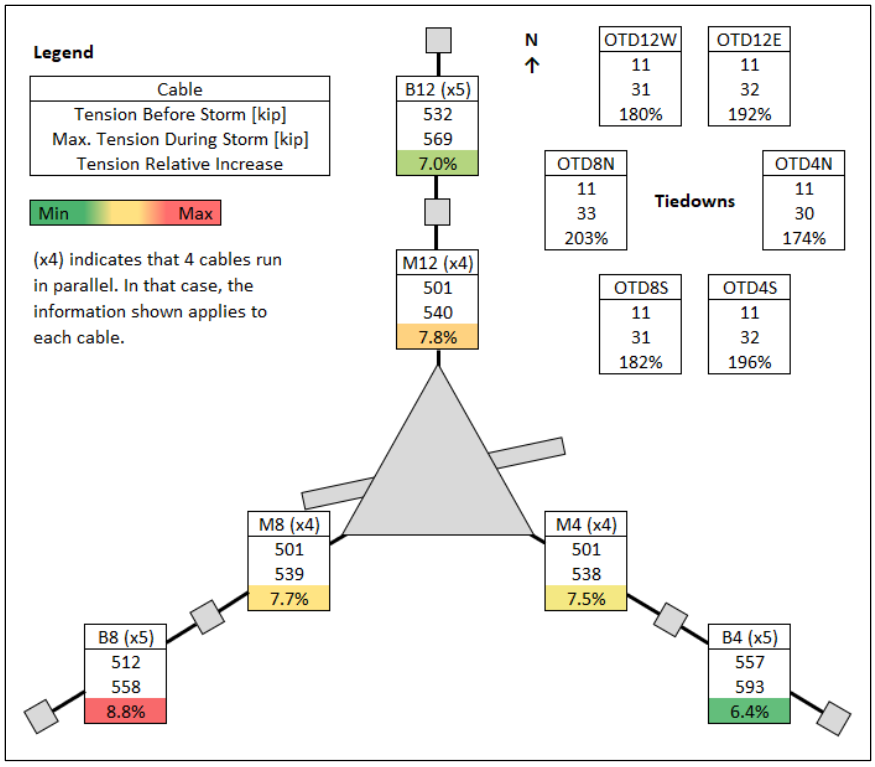

Figure 29: Maximum cable tension increase in original structure in hurricane conditions.

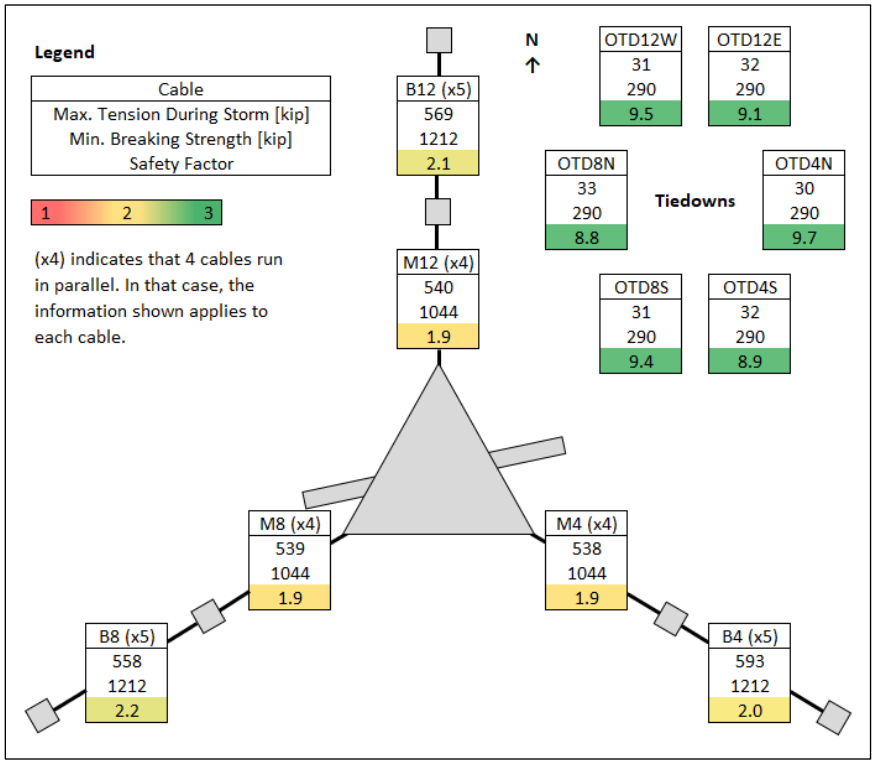

Figure 30: Maximum cable tension and corresponding safety factor in original structure in hurricane conditions.

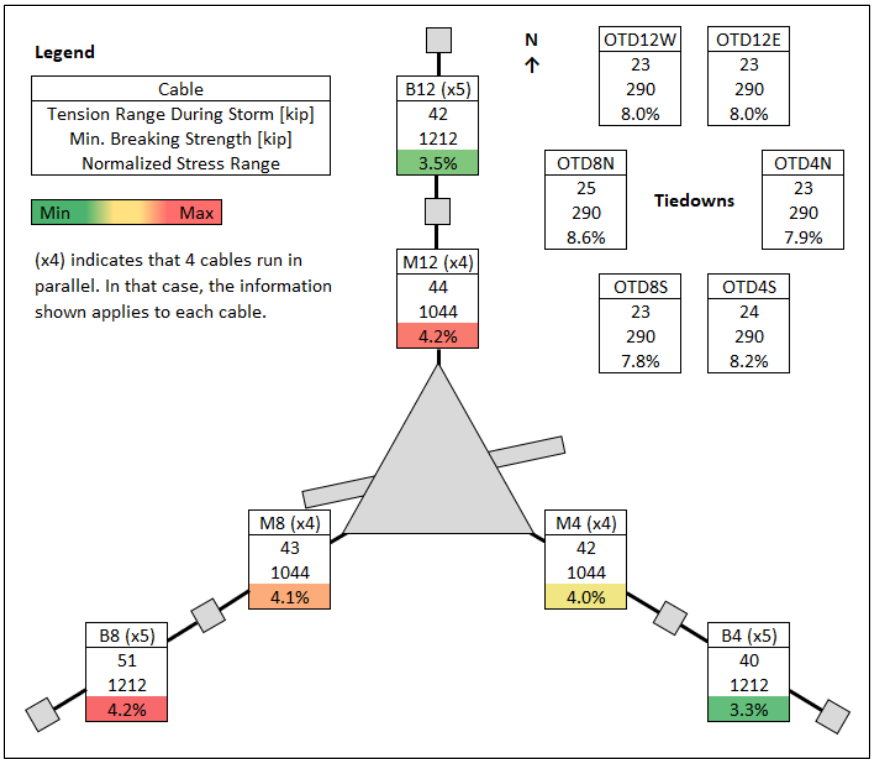

Figure 31: Maximum normalized stress range in cables of original structure in hurricane conditions.

Table 17: Number of stress cycles in cables of original structure per hour of peak hurricane conditions.

	Normalized stress range (= tension range / minimum breaking strength)			
	1-2%	**2-3%**	**3-4%**	**4-5%**
M4	66	6.1	0.3	0.1
M8	77	6.5	0.5	0.1
M12	71	5.3	0.3	0.1
B4	41	2.3	0.1	
B8	76	6.3	0.5	0.1
B12	44	2.4	0.1	

7.2 Upgraded Structure

The cable tension time histories in the upgraded structure are shown in Figure 32 for one wind direction of the ambient and hurricane conditions. For the ambient condition, the fluctuations of the cable tensions are minimal compared to the pre-existing tensions. The rest of the results presented in this section are therefore focused on the hurricane condition. The cable tension maps (Figure 33, Figure 34, Figure 35) show the envelope of the hurricane results for the three wind directions considered.

Figure 33 shows the maximum tension increase in each cable during the hurricane as a percentage of the pre-hurricane tension. The maximum tension increase is 14 percent and occurs in the three mains that support the corner of the platform where the Gregorian is stowed (M8, M4S, M12W). This is due to the significant drag-down force that the wind induces on the gregorian. The maximum tension increase in cable M4N (where the first failure occurred in August 2020) is 10 percent.

Figure 34 shows the lowest safety factor reached in each cable during the hurricane. The lowest safety factor is the ratio of the highest cable tension experienced during the hurricane to the cable's minimum breaking strength. The lowest safety factor in cable M4N is 2.1.

Figure 35 shows the maximum normalized stress range experienced by each cable during the hurricane. The maximum normalized stress range is the ratio of the maximum tension range (difference between maximum and minimum tension experienced) to the cable's minimum breaking strength. The maximum normalized stress range is around eight percent in the three cables that experience the maximum tension increase due to the drag-down force on the Gregorian.

Table 17 shows the number stress cycles experienced by each cable per hour of hurricane wind condition, for different stress levels. The number of cycles were counted in the cable tension time history results using the rainflow method, and averaged over the three wind directions considered.

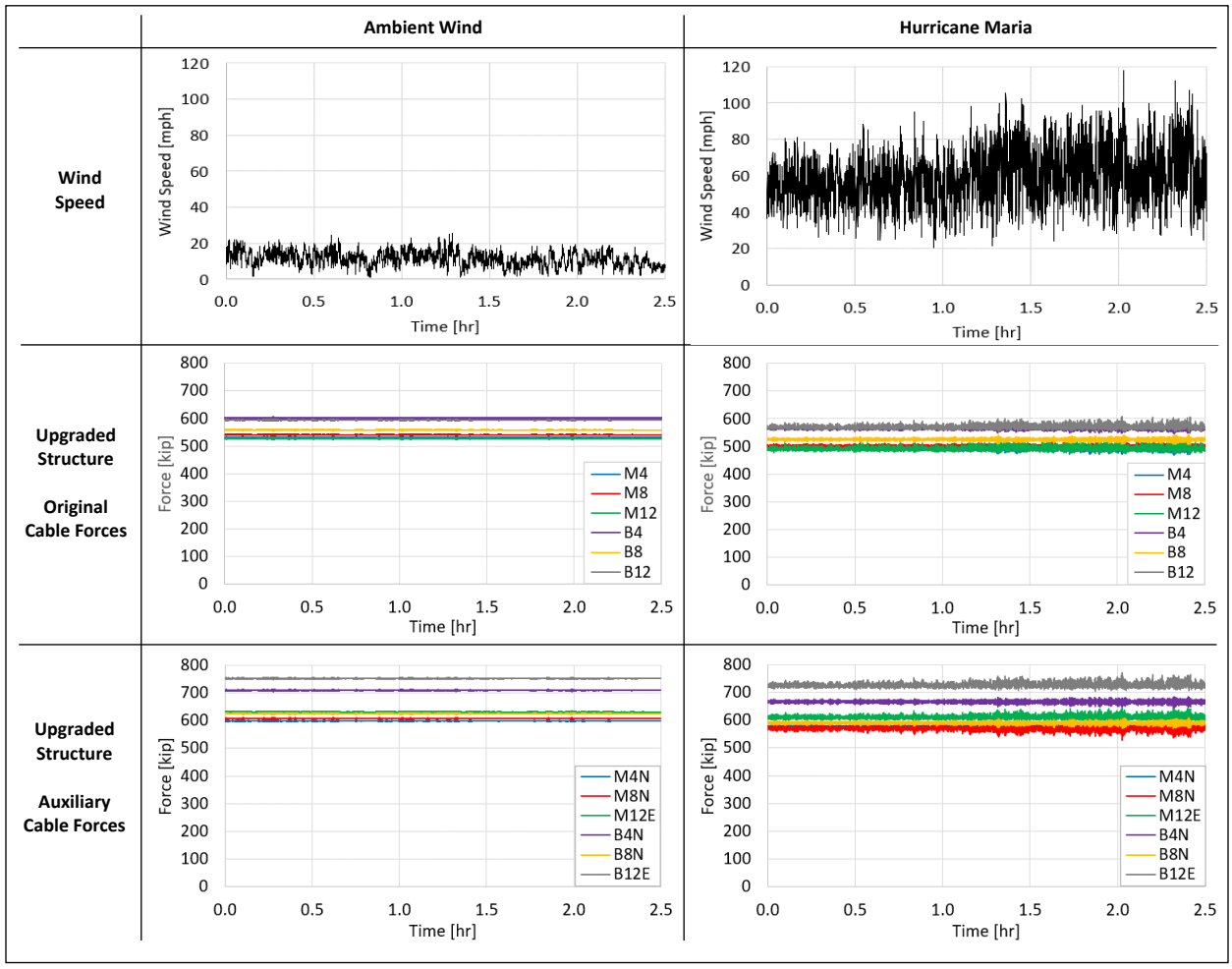

Figure 32: Cable tension time-history in original structure under ambient and hurricane wind from Tower 12 (north-south).

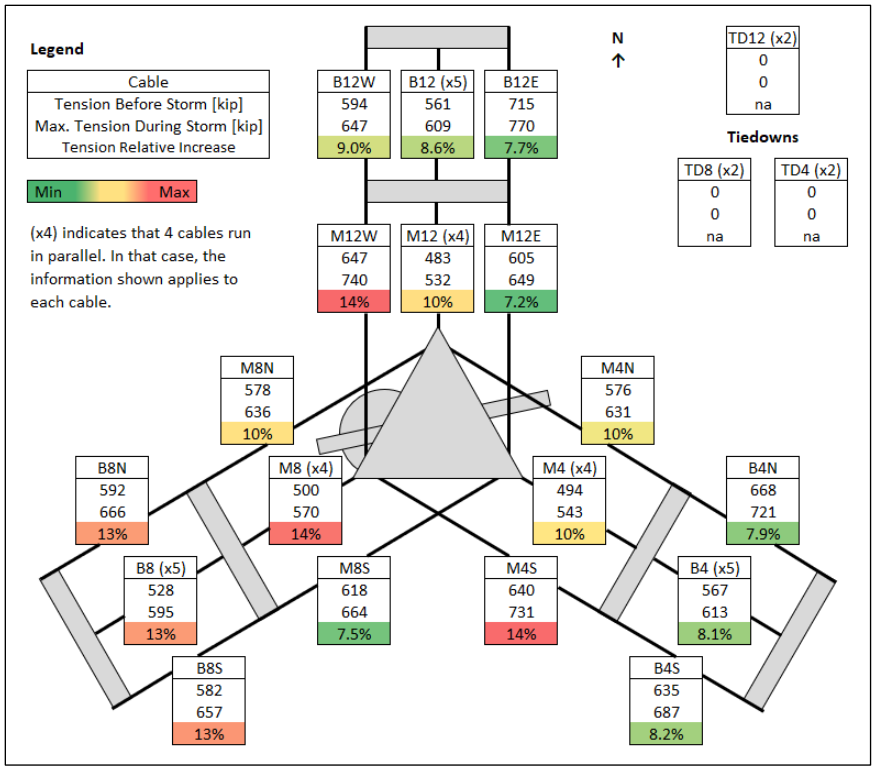

Figure 33: Maximum cable tension increase in upgraded structure in hurricane conditions.

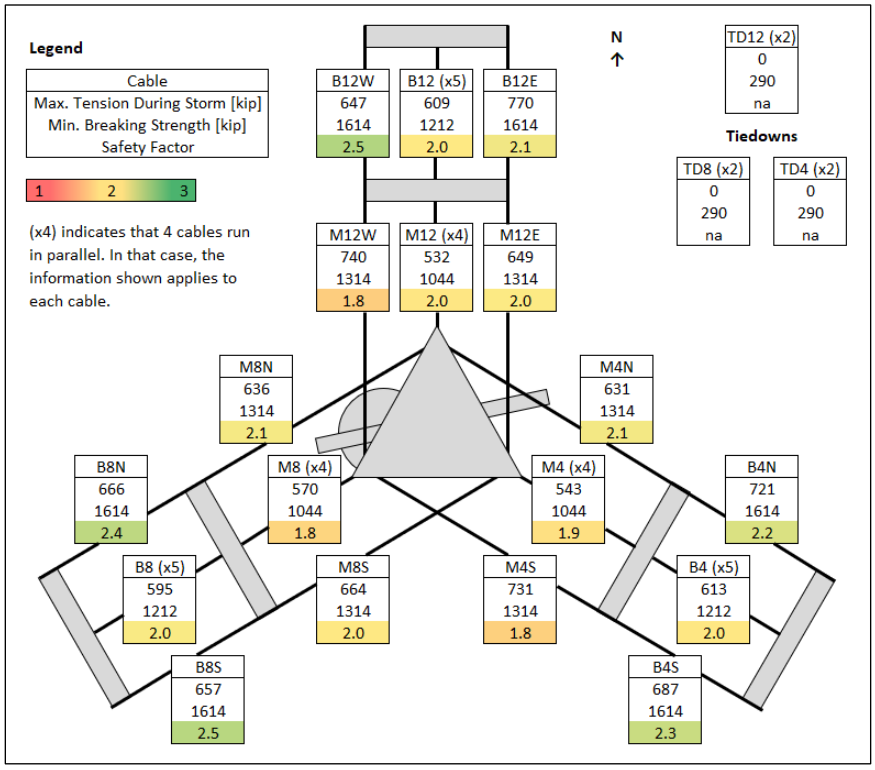

Figure 34: Maximum cable tension and corresponding safety factor in upgraded structure in hurricane conditions.

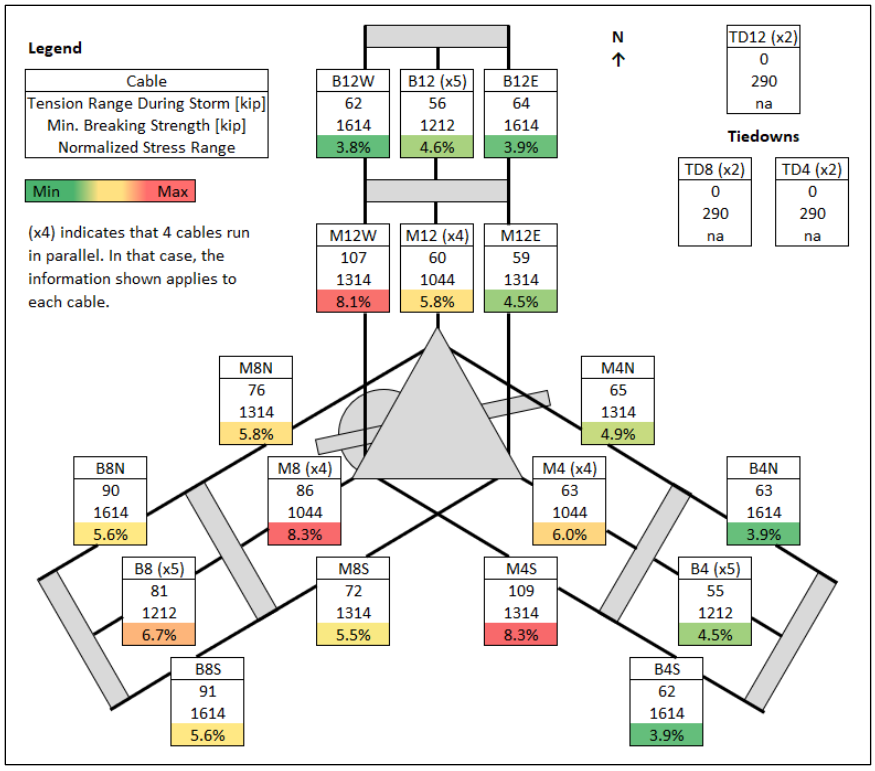

Figure 35: Maximum normalized stress range in cables of upgraded structure in hurricane conditions.

Table 18: Average number of stress cycles in cables of upgraded structure per hour of peak hurricane conditions.

	Normalized Stress Range (= Tension Range / Minimum Breaking Strength)							
	1-2%	**2-3%**	**3-4%**	**4-5%**	**5-6%**	**6-7%**	**7-8%**	**8-9%**
M4	368	101	18	3.4	0.9			
M4N	254	24	3.6	0.7				
M4S	489	114	25	7.8	1.9	1.1	0.1	0.1
M8	351	89	21	3.8	1.3	0.3	0.1	0.1
M8N	340	53	6.8	0.6	0.2			
M8S	438	96	15	1.7	0.3			
M12	352	88	19	1.9	0.7			
M12E	299	29	3.3	0.4				
M12W	473	110	20	5.7	1.5	0.3		0.1
B4	308	31	3.7	0.4				
B4N	227	16	1.6					
B4S	219	15	1.5					
B8	227	30	4.5	1.0	0.1	0.1		
B8N	158	16	1.9	0.3	0.1			
B8S	159	16	1.9	0.2	0.1			
B12	351	37	2.9	0.4				
B12E	258	14	1.3					
B12W	247	14	1.2					